

UNCLASSIFIED

AD NUMBER: AD0489311

LIMITATION CHANGES

TO:

Approved for public release; distribution is unlimited.

FROM:

Distribution authorized to U.S. Gov't. agencies and their contractors; Administrative/Operational Use; 01 Sep 1966 Other requests shall be referred to Air Force Weapons Laboratory, Kirland AFB, NM 87117

AUTHORITY

AFWAL LTR 30 NOV 1971

489311

AFWL-TR-66-51

AFWL-TR
66-51

PIEZORESISTIVE SOIL STRESS GAGES

Ernest T. Selig and Henry G. Tobin

IIT Research Institute
Chicago, Illinois

Contract AF29(601)-6628



TECHNICAL REPORT NO. AFWL-TR-66-51

September 1966

AIR FORCE WEAPONS LABORATORY
Research and Technology Division
Air Force Systems Command
Kirtland Air Force Base
New Mexico

Research and Technology Division
AIR FORCE WEAPONS LABORATORY
Air Force Systems Command
Kirtland Air Force Base
New Mexico

When U. S. Government drawings, specifications, or other data are used for any purpose other than a definitely related Government procurement operation, the Government thereby incurs no responsibility nor any obligation whatsoever, and the fact that the Government may have formulated, furnished, or in any way supplied the said drawings, specifications, or other data, is not to be regarded by implication or otherwise, as in any manner licensing the holder or any other person or corporation, or conveying any rights or permission to manufacture, use, or sell any patented invention that may in any way be related thereto.

This report is made available for study with the understanding that proprietary interests in and relating thereto will not be impaired. In case of apparent conflict or any other questions between the Government's rights and those of others, notify the Judge Advocate, Air Force Systems Command, Andrews Air Force Base, Washington, D. C. 20331.

This document is subject to special export controls and each transmittal to foreign governments or foreign nationals may be made only with prior approval of AFWL (WLDC), Kirtland AFB, N.M. Distribution of this document is limited because of the technology discussed.

BLANK PAGE

PIEZORESISTIVE SOIL STRESS GAGES

Ernest T. Selig and Henry G. Tobin

IIT Research Institute
Chicago, Illinois
Contract AF29(601)-6628

TECHNICAL REPORT NO. AFWL-TR-66-51

This document is subject to special export controls and such transmittal to foreign governments may be made only with prior approval of AFWL (WLDC), Kirtland AFB, N.M. Distribution of this document is limited because of the technology discussed.

FOREWORD

This report was prepared by the IIT Research Institute, 10 West 35th Street, Chicago, Illinois, under Contract AF29(601)-6628. The research was performed under Program Element 7.60.06.01.D, Project 5710, Subtask 13.166, and was funded by the Defense Atomic Support Agency (DASA).

Inclusive dates of research were 1 October 1964 to 31 January 1966. The report was submitted 21 June 1966 by the AFWL Project Officer, Lt Charles J. Lemont (WLDC).

The contractor's report number is M6094.

This report has been reviewed and is approved.

Charles J. Lemont

CHARLES J. LEMONT
1Lt USAF
Project Officer

Allen F. Dill

ALLEN F. DILL
CDR, CBC, USNR
Chief, Civil Engineering Branch

George C. Darby, Jr.

GEORGE C. DARBY, JR.
Colonel USAF
Chief, Development Division

ABSTRACT

A study was conducted to review the characteristics of available piezoresistive materials and evaluate their suitability as transducers for soil stress gages. The scope was limited to gages for measuring one component of static and dynamic free-field stresses. Three concepts were considered theoretically: 1) piezoresistive strain gage elements mounted on a deflecting diaphragm, 2) solid piezoresistive elements in direct compression, and 3) solid piezoresistive beam elements subjected to bending. Gages were designed and fabricated to test each of these concepts. The most satisfactory overall results were obtained with the diaphragm gage. Four such gages were delivered to AFWL in fulfillment of the contract requirements. The compression gage has merit, but there remain many fabrication problems to be overcome. Further effort will be required to develop this concept. The beam gage does not appear as practical as the other types. A systematic study of the behavior of diaphragm gages in soil is one of the most important activities that needs to be undertaken.

This page intentionally left blank.

CONTENTS

<u>Section</u>	<u>Page</u>
I. INTRODUCTION	1
II. SUMMARY	3
III. PIEZORESISTIVITY	5
1. Crystal Classification	5
2. Piezoresistive Effect	6
3. Available Materials	13
IV. GAGE CONCEPTS	15
1. Application	15
2. Gage Specifications	16
3. Deflecting Diaphragm Concept	17
4. Piezoresistive Compression Elements	22
5. Piezoresistive Bending Elements	29
6. Other Piezoresistive Gage Developments	38
V. GAGE DEVELOPMENT	43
1. Calibration Methods	43
2. Diaphragm Gage	45
3. Beam Gage	60
4. Compression Gage	65
5. UNM Gage	71
VI. FINAL DESIGN	75
1. Considerations	75
2. Description of Gage	77
3. Evaluation of Gage	80
VII. CONCLUSIONS AND RECOMMENDATIONS	85
VIII. BIBLIOGRAPHY	89
1. References Noted in Text	89
2. Other References	90
DISTRIBUTION	91

This page intentionally left blank.

ILLUSTRATIONS

<u>Figure</u>		<u>Page</u>
1	Important Planes of Cubic Crystal	7
2	Transverse Element Configuration	23
3	Cantilever Beam Gage	30
4	Thin Film Cantilever Gage	33
5	Schematic of UMM Soil Stress Gage	39
6	Schematic of WES Soil Stress Gage	40
7	Schematic of Columbia University Soil Stress Gage	41
8	Hydrostatic Calibration Apparatus	44
9	Soil Calibration Apparatus	46
10	Characteristic Gage Response Curve	47
11	Diaphragm Gage - Model I	49
12	Four-Arm Diffused Silicon Strain Gage	50
13	Hydrostatic Calibration of Model I Diaphragm Gage with Four Active Arms	53
14	Hydrostatic Calibration of Model I Diaphragm Gage with Three Active Arms	55
15	Soil Calibration of Model I Diaphragm Gage with Three Active Arms	57
16	Diaphragm Gage - Model IA	58
17	Hydrostatic Calibration of Model IA Diaphragm Gage	59
18	Soil Calibration of Model IA Diaphragm Gage	61
19	Beam Gage - Model III	62
20	Hydrostatic Calibration of Model III Beam Gage	64
21	Soil Calibration of Model III Beam Gage	66

ILLUSTRATIONS, Cont'd

<u>Figure</u>		<u>Page</u>
22	Compression Gage - Model II	67
23	Soil Calibration of Model II Compression Gage	70
24	Response of Silicon Element in Direct Compression	72
25	Hydrostatic Calibration of UNM Soil Stress Gage	73
26	Soil Calibration of UNM Soil Stress Gage	74
27	Summary of Gage Response in Soil	76
28	Diaphragm Gage Model IB	78
29	Final Gage Design - Model IB	81
30	Hydrostatic Calibration of Model IB Diaphragm Gage	82
31	Soil Calibration of Model IB Diaphragm Gage	83

TABLES

<u>Table</u>		<u>Page</u>
I	Translated Piezoresistance Coefficients	12
II	Piezoresistive Coefficients	25
III	Transverse Piezoresistive Coefficient	26
IV	Piezoresistive Coefficients	28
V	Physical Characteristics of Gages Tested	52
VI	Representative Gage Calibration Data	54

This page intentionally left blank.

NOTATION

A	Cross-sectional area of strain gage or beam
E_1	Electric field, volts/unit length
F	Concentrated force
I_j	Current density, amps/unit area
J	Coefficient
K	Gage factor
L	Length of strain gage or beam
R	Resistance
T_{ij}	Stress tensor, force/unit area
Y	Young's modulus
a	Radius of diaphragm
b	Width of beam
g	Acceleration due to gravity
m	Direction cosine
n	Direction cosine
r	Radial distance from center of diaphragm
t	Thickness of diaphragm or beam
w	Distributed pressure on diaphragm
x	Direction coordinate
y	Direction coordinate
y_c	Center deflection of clamped diaphragm
l	Direction cosine
α	Coefficient
β	Direction cosine
γ	Weight density of diaphragm material

NOTATION, Contd

δ	Kronecker delta
e	Strain
e_c	Strain at center of diaphragm
e_r	Radial strain on diaphragm
θ	Direction cosine
ν	Poisson's ratio
π_{ijkl}	Piezoresistive coefficient
ρ	Resistivity

SECTION I

INTRODUCTION

Civil Engineers have been interested in free-field soil stress measurements for at least 50 years. The Goldbeck cell, one of the first to be widely used, was reported in the literature in 1916. The earliest gages were bulky and suitable only for the measurement of static pressures in large earth masses. Over the years, the development of new instrumentation techniques has permitted the achievement of more compact gages with shorter response times.

More recently, because of the need to measure shock response, piezoelectric materials have become popular as a transducer element. They were first used for fluid pressure gages and were limited to very short duration pulses because of the capacitive nature of the circuitry. With new instrumentation, piezoelectric gages are now being used for slowly varying stress measurements in soil. They have found frequent application in the laboratory because of their adaptability to miniaturization. However, because of problems when using long leads and their considerable sensitivity to temperature, electromagnetic and moisture effects, they have not yet found wide application in the field.

A relatively new piezoresistive semiconductor material, which appears to offer a number of advantages over piezoelectric and other transducers, is now commercially available. The potential of this material has been relatively unexplored as a stress gage element, except for applications in the form of thin strain gage elements. Such transducers have the advantage of a much higher sensitivity over foil and wire strain gages. There are, however, many other features of this material that make it attractive as a stress gage transducer. Among these are the relatively simple instrumentation requirements (i.e., resistance bridge) and the suitability for both static and dynamic measurements. In addition, there are special resistance characteristics such that both positive and negative resistance changes can be obtained for the same stress and thermal

effects and the elements can be made sensitive only to certain components of stress. Finally, the material can be fabricated in virtually any shape and size.

The purpose of this study is to evaluate the feasibility of using piezoresistive semiconductors as transducers for soil stress gages. Attention is primarily being devoted to single function free-field stress gages, i.e., one component of normal stress, shear stress or pore pressure with emphasis on normal stress measurement. The investigation contains four phases: 1) a review of published literature and information available from manufacturers to determine the properties, behavior, size and cost of piezoresistive materials; 2) a theoretical evaluation of the behavior of piezoresistive materials to determine their sensitivity to various stress components and to establish the proper transducer size and shapes; 3) design, fabrication, and testing of gages using the most promising concepts; and, 4) fabrication and delivery to AFWL of four gages of the most successful design. The accomplishments of each of these phases are discussed in this report.

SECTION II

SUMMARY

Recent developments in semiconductor technology have made available a variety of piezoresistive materials that appear to have value as transducers for gages to measure stress in soil.

The theoretical behavior of piezoresistive materials has been found to be well documented in the literature. A survey of manufacturers was made to determine what materials were available and to obtain data describing their properties. On the basis of this information a number of potential concepts were evaluated theoretically so that the most promising approaches could be selected. Attention was restricted to the measurement of a single component of normal stress in soil. The applications considered theoretically were: 1) commercial piezoresistive strain gages mounted on diaphragms subjected to soil pressure; 2) solid piezoresistive elements subjected to direct compression by the soil stress; and, 3) beam elements subjected to bending under concentrated loading from the soil. In the third case the beams considered were either solid piezoresistive material or steel with commercial piezoresistive strain gages mounted on them. Specific gages were designed to permit experimental evaluations of these concepts including determination of the practical difficulties in their fabrication.

Fabrication difficulties were encountered with all three concepts, but the major problems were associated with the solid piezoresistive elements. The raw materials were found to be readily available, however, the elements themselves had to be fabricated by ITRI. This was a difficult task and little information was available to provide assistance. Techniques were finally developed for fabricating these elements so that a direct compression gage could be constructed. The solid piezoresistive beam element was not fabricated, however.

The gages constructed were evaluated under a uniform hydrostatic pressure and buried in confined samples of sand. In both cases static pressures up to 500 psi were applied and released. For comparison, a piezoresistive soil stress gage, the University of New Mexico (UNM) gage, developed at the Eric H. Wang Civil Engineering Research Facility (CERF) was evaluated in the same manner.

The gage, whose overall performance was best, utilized the deflecting-diaphragm concept. The results demonstrated that a gage of this type, whose performance is reasonably linear in soil with a small amount of hysteresis and has a registration ratio (response in soil divided by response under hydrostatic pressure) near 1, can be constructed.

The compression gage behaved erratically, and although considerable development effort was expended on this concept, the problems were not eliminated. Mechanical difficulties were encountered with the beam gage. These could be overcome, but the concept did not appear to have sufficient value in relation to the others considered to justify further attention. The UNM gage performed linearly with little hysteresis in soil but appeared to be quite sensitive to the placement conditions and generally overregistered by a large amount.

On the basis of the study a stress gage was designed, using a dual element commercial piezoresistive strain gage mounted on a 0.75-in. diameter by 0.10-in. thick diaphragm. The entire gage was machined from aluminum to aid in matching its density to that of the soil. The overall gage size was 1.5 in. in diameter by 0.225 in. thick. The two active arms were matched with fixed resistors inside of the gage case in order to provide a four-arm balanced bridge. The research results suggest that, with additional development, the performance of this gage concept can be further improved. The effort most needed at the present is a thorough evaluation of this gage in soil with a systematic variation of the controlling parameters.

SECTION III

PIEZORESISTIVITY

A literature survey was conducted to obtain information on the piezoresistive effect in materials, as well as previous transducer work, which had been carried out using these materials. A bibliography of those articles that were found to be of most use on the program is included at the end of this report.

The piezoresistance phenomenon is the name given to the effect wherein a material exhibits a change in resistivity due to an applied stress. The change in resistance of a specimen of such material is much greater than can be attributed to a change in its dimensions alone. In those materials in which the piezoresistive effect is large, the change in resistance due to dimensional changes may generally be neglected in comparison to the changes due to the piezoresistive effect. The first piezoresistance measurements were made in 1925 by Bridgman (Ref 1). The results reported by Bridgman were carried out on several polycrystalline metals. The effect noted was generally small. Of most interest for present applications of the piezoresistive effect are the results given by Smith (Ref 2). He was the first to report the piezoresistive coefficients for cubic crystals, namely germanium and silicon. In order to make clearer the discussion to follow, a review of some of the properties of crystals will be given.

1. CRYSTAL CLASSIFICATION

Crystals may be categorized according to their symmetry properties. When the lattice constants along the three axes are equal and when the axes form right angles with each other, the crystal is said to be cubic. The piezoresistive effect has been studied most extensively in such crystals. The following description will be restricted, therefore, to cubic crystals.

The position and orientation of a crystal plane is determined by giving the coordinates of the points at which the plane intersects the crystal axes. Miller indices are generally used to

specify the orientation. These indices are obtained by first determining the intercepts of the plane on the axes. The reciprocals of these numbers are taken and reduced to the smallest three integers having the same ratio. The result of this operation is enclosed in parentheses.

Suppose a plane intersects the axes at the points (100), (020) and (004). The reciprocals of the intercepts are 1, 1/2 and 1/4. The Miller indices are, therefore, (421). If the intercept is at infinity, the corresponding Miller index is zero. If the plane intercepts the axis on the negative side of the origin, the corresponding index is negative and is indicated by placing a minus sign above the index, e.g., ($\bar{4}$ 21). Planes that are equivalent by symmetry or a family of planes are denoted $\{421\}$. Directions are also indicated by indices. A direction uvw is perpendicular to a plane uvw having the same indices. Directions are denoted by $[uvw]$, while equivalent directions or a family of directions are denoted by $\langle uvw \rangle$. Figure 1 shows a cubic crystal and some of the important planes of this crystal.

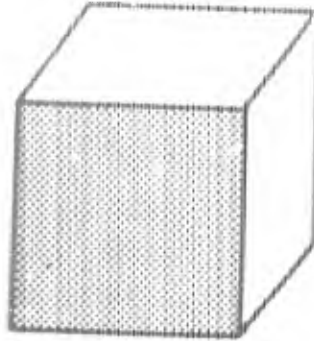
2. PIEZORESISTIVE EFFECT

The piezoresistive effect describes the change in resistance of certain crystals when subjected to stress or strain. Consider that an electric field is applied to such a crystal. Assume that the electric field components, E_i (volt/unit length), are functions of the current density components, I_j (amp/unit area), and the stress components T_{kl} . By employing the technique used by Mason and Thurston (Ref 3), the following basic piezoresistive equation may be derived

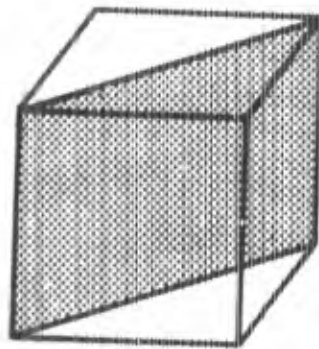
$$E_i = \rho_{ij} I_j + \pi_{ijkl} I_j T_{kl} \quad (1)$$

The first term, $\rho_{ij} I_j$, represents the semiconductor counterpart of Ohm's law. The second term, $\pi_{ijkl} I_j T_{kl}$, represents the piezoresistive effect where $\pi_{ijkl} T_{kl}$ is the change in resistance due to the application of stress. The piezoresistive coefficient π_{ijkl} is a fourth order tensor consisting in general of 81 components.

(100)



(110)



(111)

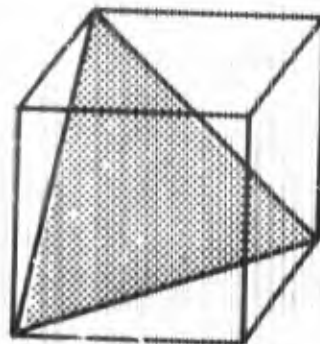


Figure 1. Important Planes of a Cubic Crystal

It can be shown that in general for cubic crystals

$$\begin{aligned} \pi_{ijkl} &= \pi_{jikl} \\ &= \pi_{jilk} \\ &= \pi_{ijlk} . \end{aligned} \tag{2}$$

This reduces the number of components to 36. The equality given by Eq (2) permits the first two subscripts to be interchanged and the last two subscripts to be interchanged. In order to simplify the notation, one may, therefore, substitute a single numeral for the first pair of subscripts and for the second pair of subscripts. The following notation is used:

$$\begin{aligned} 11 &\longrightarrow 1 , \\ 22 &\longrightarrow 2 , \\ 33 &\longrightarrow 3 , \\ 23 &\longrightarrow 4 , \\ 13 &\longrightarrow 5 , \\ 12 &\longrightarrow 6 . \end{aligned}$$

This same substitution may be used for the stress components. Thus, the stress tensor can be designated by a single subscript while the piezoresistive coefficient can be designated by a double subscript.

Unstressed silicon and germanium exhibit a cubic, i.e., symmetric, crystal structure in which

$$\begin{aligned} \rho_1 &= \rho_2 = \rho_3 = \rho_0 , \\ \rho_4 &= \rho_5 = \rho_6 = 0 . \end{aligned} \tag{3}$$

Hence Eq (1) may be written

$$E_i = \rho_0 I_i + \pi_{ijkl} I_j T_{kl} . \tag{4}$$

In addition, for cubic crystals only three independent piezoresistive coefficients are nonzero. These are π_{1111} , π_{1122} and π_{2323} which may be written as $\rho_0 \pi_{11}$, $\rho_0 \pi_{12}$ and $\rho_0 \pi_{44}$ respectively using the simplified notation and factoring out a constant ρ_0 .

After some manipulation and use of the stated conditions the following basic piezoresistive equations may be derived from Eq (4) for cubic crystals.

$$\frac{E_1}{\rho_0} = I_1 [1 + \pi_{11}T_1 + \pi_{12}(T_2 + T_3)] + \pi_{44} [I_2T_6 + I_3T_5] ,$$

$$\frac{E_2}{\rho_0} = I_2 [1 + \pi_{11}T_2 + \pi_{12}(T_1 + T_3)] + \pi_{44} [I_1T_6 + I_3T_4] , \quad (5)$$

$$\frac{E_3}{\rho_0} = I_3 [1 + \pi_{11}T_3 + \pi_{12}(T_1 + T_2)] + \pi_{44} [I_1T_5 + I_2T_4] .$$

The subscripts 1, 2, and 3 on E and I indicate orientations coincident with the principal axes of the crystal, and the subscripts on π and T are based upon the simplified notation.

Two interesting effects may be observed:

1. If the current and voltage are taken in the same direction and there is no current in the other two directions, then only the three normal stresses will influence the output.
2. If the current and voltage are taken at right angles, say orientations 1 and 2, then only the one component of shear stress T_6 will influence the output.

In order to analyze any general crystal orientation, a new Cartesian coordinate system with axes 1', 2' and 3' is required. Let the transformation between this system and the crystal axes be given by the matrix on the next page, where l , m , and n are the direction cosines between the appropriate axes.

		Crystal Axis		
		1	2	3
Coordinate System Axis	1'	l_1	m_1	n_1
	2'	l_2	m_2	n_2
	3'	l_3	m_3	n_3

The current in the direction of the crystal axes is given by

$$I_m = \sum_{p=1}^3 \beta_p I_p' , \quad (6)$$

where β_p is the direction cosine l , m , or n associated with the subscript m direction ($m = 1, 2, \text{ or } 3$). A stress is given in double subscript form by

$$T_{mn} = \sum_{p=1}^3 \left[\beta_p \theta_p T_{pp}' + \sum_{q=1}^3 \beta_p \theta_q T_{pq}' (1 - \delta_{pq}) \right] \quad (7)$$

where T_{mn} is the stress with respect to the crystal axes, β_p is defined as before, θ is the direction cosine associated with the subscript n direction, and δ_{pq} , called Kronecker delta, is equal to zero for $p \neq q$ and equal to one for $p = q$. The electric field components in the rotated system are given by

$$\begin{bmatrix} E_1' \\ E_2' \\ E_3' \end{bmatrix} = \begin{bmatrix} l_1 & m_1 & n_1 \\ l_2 & m_2 & n_2 \\ l_3 & m_3 & n_3 \end{bmatrix} \begin{bmatrix} E_1 \\ E_2 \\ E_3 \end{bmatrix} \quad (8)$$

By substitution of Eq (6) and (7) into Eq (8) and the resulting expressions substituted into Eq (5) the relationship between the electric field, the resistivity, the current, and the stress is determined (Ref 4). It is of the form

$$\begin{aligned}
 E_1'/\rho_0 = & I_1' \left(1 + \pi_{11}'T_1' + \pi_{12}'T_2' + \pi_{13}'T_3' + \pi_{14}'T_4' \right. \\
 & \left. + \pi_{15}'T_5' + \pi_{16}'T_6' \right) \\
 & + I_2' \left(\pi_{61}'T_1' + \pi_{62}'T_2' + \pi_{63}'T_3' + \pi_{64}'T_4' \right. \\
 & \left. + \pi_{65}'T_5' + \pi_{66}'T_6' \right) \\
 & + I_3' \left(\pi_{51}'T_1' + \pi_{52}'T_2' + \pi_{53}'T_3' + \pi_{54}'T_4' \right. \\
 & \left. + \pi_{55}'T_5' + \pi_{56}'T_6' \right) ,
 \end{aligned} \tag{9}$$

where the stress components are written in single subscript form. Analogous expressions may be written for E_2'/ρ_0 and E_3'/ρ_0 .

In order to analyze any general orientation, it is necessary to determine the value of the primed piezoresistive coefficients in terms of the unprimed coefficients. This may be done in several ways. One of these is to apply the rules of tensor transformations to the unprimed coefficients. Alternately, Eq (6), (7) and (8) may be used to derive Eq (9) in terms of the unprimed coefficients and the direction cosines of the transformation used. The primed piezoresistive coefficients may then be determined by an examination of the appropriate coefficient in the expressions for the primed electric field components in terms of the primed stress and current components. As an example, π_{46}' would be the coefficient of $I_3'T_6'$ in the expression for E_2' . For cubic crystals, $\pi_{ab} = \pi_{ba}$. Therefore, 18 independent piezoresistive coefficients may be written in the primed coordinate system. These 18 coefficients are given in Table I.

Equation (9) and Table I together provide the general relationships between current, voltage field, stress, and piezoresistive coefficients for any arbitrary orientation in symmetric crystals.

Table I
TRANSLATED PIEZORESISTANCE COEFFICIENTS (Ref 4)

$$\begin{aligned}
 \pi_{11}' &= \pi_{11} - 2 (\pi_{11} - \pi_{12} - \pi_{44}) [(l_1 m_1)^2 + (m_1 n_1)^2 + (n_1 l_1)^2] \\
 \pi_{22}' &= \pi_{11} - 2 (\pi_{11} - \pi_{12} - \pi_{44}) [(l_2 m_2)^2 + (m_2 n_2)^2 + (n_2 l_2)^2] \\
 \pi_{33}' &= \pi_{11} - 2 (\pi_{11} - \pi_{12} - \pi_{44}) [(l_3 m_3)^2 + (m_3 n_3)^2 + (n_3 l_3)^2] \\
 \pi_{44}' &= \pi_{44} + 2 (\pi_{11} - \pi_{12} - \pi_{44}) [(l_2 l_3)^2 + (m_2 m_3)^2 + (n_2 n_3)^2] \\
 \pi_{55}' &= \pi_{44} + 2 (\pi_{11} - \pi_{12} - \pi_{44}) [(l_1 l_3)^2 + (m_1 m_3)^2 + (n_1 n_3)^2] \\
 \pi_{66}' &= \pi_{44} + 2 (\pi_{11} - \pi_{12} - \pi_{44}) [(l_1 l_2)^2 + (m_1 m_2)^2 + (n_1 n_2)^2] \\
 \pi_{12}' &= \pi_{12} + (\pi_{11} - \pi_{12} - \pi_{44}) [(l_1 l_2)^2 + (m_1 m_2)^2 + (n_1 n_2)^2] \\
 \pi_{13}' &= \pi_{12} + (\pi_{11} - \pi_{12} - \pi_{44}) [(l_1 l_3)^2 + (m_1 m_3)^2 + (n_1 n_3)^2] \\
 \pi_{14}' &= \pi_{56}' = 2 (\pi_{11} - \pi_{12} - \pi_{44}) [l_1^2 l_2 l_3 + m_1^2 m_2 m_3 + n_1^2 n_2 n_3] \\
 \pi_{15}' &= 2 (\pi_{11} - \pi_{12} - \pi_{44}) [l_1^3 l_3 + m_1^3 m_3 + n_1^3 n_3] \\
 \pi_{16}' &= 2 (\pi_{11} - \pi_{12} - \pi_{44}) [l_1^3 l_2 + m_1^3 m_2 + n_1^3 n_2] \\
 \pi_{23}' &= \pi_{12} + (\pi_{11} - \pi_{12} - \pi_{44}) [(l_2 l_3)^2 + (m_2 m_3)^2 + (n_2 n_3)^2] \\
 \pi_{24}' &= 2 (\pi_{11} - \pi_{12} - \pi_{44}) (l_2^3 l_3 + m_2^3 m_3 + n_2^3 n_3) \\
 \pi_{25}' &= \pi_{46}' = 2 (\pi_{11} - \pi_{12} - \pi_{44}) (l_1 l_2^2 l_3 + m_1 m_2^2 m_3 + n_1 n_2^2 n_3) \\
 \pi_{26}' &= 2 (\pi_{11} - \pi_{12} - \pi_{44}) (l_1 l_2^3 + m_1 m_2^3 + n_1 n_2^3) \\
 \pi_{34}' &= 2 (\pi_{11} - \pi_{12} - \pi_{44}) (l_2 l_3^3 + m_2 m_3^3 + n_2 n_3^3) \\
 \pi_{35}' &= 2 (\pi_{11} - \pi_{12} - \pi_{44}) (l_1 l_3^3 + m_1 m_3^3 + n_1 n_3^3) \\
 \pi_{36}' &= \pi_{45}' = 2 (\pi_{11} - \pi_{12} - \pi_{44}) (l_1 l_2 l_3^2 + m_1 m_2 m_3^2 + n_1 n_2 n_3^2)
 \end{aligned}$$

From these relationships, orientations giving maximum sensitivity as well as those in which certain coefficients are zero may be determined. Such situations are discussed by Pfann and Thurston (Ref 4). Appropriate cases will be examined later in this report in connection with specific gage designs.

3. AVAILABLE MATERIALS

In order that usable gages might be designed, it was decided to initiate the program with a survey that would include both the literature and various manufacturers to determine what work had been carried out in the past and to determine also what piezoresistive materials would be readily available. Forty-seven manufacturers, who might possibly be suppliers of piezoresistive materials, were contacted. Four suppliers of commercial piezoresistive strain gages were also contacted. In addition, a letter was sent to the Germanium Information Center, inquiring about information available concerning the piezoresistive properties of that material.

Twenty-eight of the manufacturers replied to the letter concerning basic semiconductor materials. Four gage manufacturers replied. The following gives a summary of the responses received from the material suppliers. The summary will be given in rather general terms since the rapid advances in semiconductor technology may have caused certain of the manufacturers to revise the materials and types that they are willing or able to supply.

The most commonly available material is n- or p-type silicon. Usually only one resistivity is available as an off-the-shelf item. Some manufacturers were also willing to supply n- and p-type germanium, usually in only one resistivity without a special order. In bulk form, the material was generally available in a rod configuration with the axis of the rod being in the [111] direction. Most of the responders who were willing to supply the material would not quote prices without specific details concerning the material desired. This indicated that each order was filled on a special basis, causing the price of the material to be rather high.

Most of the commercial strain gages available were of the same type, namely a slice of silicon on a glass-epoxy carrier. Two manufacturers, however, offer diffused silicon gages on a substrate, which is bulk silicon. These gages may be placed in position by means of soldering or welding. Only one commercial strain gage, which consisted of both an n- and p-type gage on a single backing, was offered. This gage should give changes in resistance in each of its elements, which are opposite in sign, as a function of the applied strain. The gage factors available ranged from -140 to 170, with resistance of between 60 and 10,000 ohms.

SECTION IV

GAGE CONCEPTS

1. APPLICATION

The current state-of-the-art of soil stress measurement suggests that a universal soil stress gage is not feasible. This is primarily the result of the complex nature of soil stress-strain relationships. The proper gage design must therefore be based upon the particular application taking into consideration such factors as the type of stress (e.g., normal, hydrostatic, or shear), magnitude of stress, stress-strain characteristics of the soil, whether the application is free-field or at soil-structure interfaces, and finally, the environmental conditions such as temperature, radiation, and moisture conditions.

The transducer and the environmental conditions may be the same in the free-field as for measurements at soil-structure interfaces, but the gage design and configuration may be entirely different in the two cases. For both applications, normal stress, shear stress, and pore pressure are of interest and several components of each or combinations such as normal and shear stress may be desired. However, the successful measurement of single components of stress is still sufficiently unresolved that it is best to avoid the further complication of attempting combination measurements in soil. A review of piezoresistive theory indicates that from electronic considerations alone, it is possible to simultaneously measure several stress components with a single element by proper application of current and measurement of voltage; however, from a soil-gage interaction point of view it does not appear that these components can be related to the desired free-field values. Therefore, in the present study the primary emphasis is placed upon the measurement of a single component of free-field stress, specifically normal stress.

A number of factors must be considered in the overall gage design and the selection of a transducer. The existence of a complex stress field in the soil must be assumed. In order to

measure a single component of stress, the influence of the other components of stress on the gage must be minimized. The gage must be adequately waterproof and not be significantly affected by other environmental factors such as temperature and radiation. For most soil applications temperature has not been a major problem as long as compensation for long term temperature changes is provided. The rate of change of stress, i.e., static or dynamic application, is important because it affects the requirements of the instrumentation, the gage frequency response and the density matching with the soil.

2. GAGE SPECIFICATIONS

Based upon the foregoing discussion and review of current theories of soil stress measurement (Ref 5) , the following nominal specifications were selected as a basis for the design of a normal stress gage for free-field soil application:

- Disk-shaped with small thickness-diameter ratio, say $\leq 1/10$ (stress component to be measured is normal to face of disk).
- Gage diameter between 1 and 2 in. (gage size is important with respect to soil conditions, type of sensing element, and size of test specimen).
- Overall gage stiffness as high as possible, say equivalent to a diaphragm diameter-deflection ratio $\geq 5,000$.
- Overall gage density in the same range as that of soil, say 110 to 140 lb/cu ft.
- Frequency response suitable for application between dc and 10,000 cps.
- Active sensing area less than total area of gage face, say 50 percent.
- Stress measurement in the range of zero to 500 psi.

- Compatability with low impedance conventional recording instruments and the use of long leads, say up to 100 ft.
- Long term temperature compensation.
- Adequately waterproofed for embedment in soil over a period of days.
- Capable of being calibrated in terms of the true free-field soil stress with satisfactory linearity and hysteresis characteristics.

It is recognized that it may not be possible to meet all criteria simultaneously so that some compromise must be made. However, preliminary guidelines are necessary as a basis against which to evaluate each potential concept.

Two basic directions of approach for transducer design were considered, one using the commercial semiconductor strain gage elements and the other using solid piezoresistive crystals in compression or bending. It does not appear that the latter concept has been considered previously for soil stress gage design. Several applications of the former concept are being considered by other investigators. These will be discussed later. The objective of this evaluation phase is to select the most promising directions of approach prior to fabricating and testing any specific concepts.

3. DEFLECTING DIAPHRAGM CONCEPT

The simplest type of gage that can be envisioned is one that uses a circular diaphragm clamped at the edges. The pressure on the diaphragm is related to the output of strain gages mounted on the diaphragm. For a flat plate of radius "a" (in.), with a uniformly distributed load, w(psi), the strain at the center e_c is given by (Ref 6)

$$e_c = \frac{3}{8} \frac{a^2 w}{Yt^2} (1 - \nu^2) , \quad (10)$$

where

ν = Poisson's ratio,

t = thickness, in.,

Y = Young's modulus, psi,

and w has been taken as positive, and tensile strains are positive.

Optimum linearity is obtained if the strain on semiconductor gages is held to within $\pm 1000\mu$ in./in. The gage factor (K) is defined by

$$K = \frac{\Delta R}{R_0 \epsilon}, \quad (11)$$

where

R_0 = the nominal resistance,

ΔR = the change in resistance because of strain ϵ .

Commercial semiconductor gages have gage factors of 100 or higher. A strain of 1000μ in./in. would, therefore, give a change in resistance of 10 percent.

At any point on the diaphragm, the radial strain is given (Ref 6) by

$$\epsilon_r = \frac{-3w(1 - \nu^2)}{8Yt^2} (3r^2 - a^2), \quad (12)$$

where

r = radial distance from the center of the diaphragm to any point on the diaphragm.

The maximum radial strain occurs at the circumference and is given (Ref 6) by

$$\epsilon_{r_{\max}} = \frac{-3a^2w}{4Yt^2} (1 - \nu^2). \quad (13)$$

The change in resistance of a gage placed in a radial direction will depend upon its length and its distance from the center of the diaphragm. It can be seen from Eq (12) that the strain changes sign, i.e., changes from a tensile to a compressive strain, as a radial line is traversed. The total change in resistance, therefore, will depend upon whether the gage crosses the point of zero strain.

For a given gage, the resistivity ρ will be of the form

$$\rho = \rho_0 (1 + K\varepsilon) \quad , \quad (14)$$

where

ρ_0 = nominal resistivity,

K = gage factor.

Since

$$R = \frac{\rho L}{A} \quad , \quad (15)$$

where

R = resistance of the gage,

L = length of the gage,

A = cross-sectional area of the gage element,

the change in resistance of a radial gage may be found from

$$\Delta R = \int_{r_1}^{r_2} \frac{\rho_0 K\varepsilon}{A} dr \quad , \quad (16)$$

where ε is given by Eq (12) and r_2, r_1 are the radial positions of the two ends of the gage ($r_2 > r_1$). For the case where the gage is placed as near the edge of the diaphragm as possible, the limits of the integral in Eq (16) become $a-L$ and a , where L is the total length of the gage. If the gage is placed so that its center coincides with the center of the diaphragm, the integration can be carried out between zero and $L/2$. The total resistance will be twice the value given by this integration.

By substituting Eq (12) into Eq (16) and integrating, the change in resistance for these two cases can thus be shown to be

$$\Delta R_e = K_1 (a - L) \left[1 - \left(\frac{a - L}{a} \right)^2 \right], \quad (17)$$

$$\Delta R_c = K_1 L \left[\left(\frac{L}{2a} \right)^2 - 1 \right], \quad (18)$$

where

$$K_1 = \frac{3}{8} \frac{\rho_o}{A} K \frac{wa^2}{Yt^2} (1 - \nu^2),$$

ΔR_e = change in resistance of gage placed at edge,

ΔR_c = change in resistance of gage placed at center.

Since the gage will be in tension at the center of the diaphragm and in compression at the edge, the change in resistance will be of opposite sign at these two positions. This is an ideal situation for a bridge application.

The magnitude of the changes is of interest. From Eq (17) and (18) it can be shown that for

$$L = \frac{2}{5} a, \quad (19)$$

the magnitude of the resistance change is the same for gages centered on the diaphragm and radial gages with one end at the edge of the diaphragm. If the gage length is shorter than given by Eq (19), the change in resistance at the edge will be greater than that at the center; while for L greater than the value given by Eq (19), the situation will be reversed. Thus, the optimum placement of the gage will depend upon the length of the gage as compared to the radius of the diaphragm.

If the gage is to be used in a bridge circuit, the ratio of the output voltage of the bridge to the input voltage can be made equal to the ratio of resistance change of one arm of the bridge to the unstrained resistance if a four-active-arm bridge

is used and adjacent arms are made to change equally but in the opposite sense. This could be accomplished if two gages were placed across the center of the diaphragm and two near the edge. The exact placement of the gages near the edge should be selected so as to make the total resistance change of the edge-placed gages equal to those across the center of the diaphragm. By using Eq (16), an expression for r_2 or r_1 in terms of the length of the gage and the radius of the diaphragm can be derived for the condition of equal but opposite resistance changes for a given gage near the edge of the disk or across the center of the disk. This expression, in terms of r_2 , is given by

$$r_2 = \frac{3L + \sqrt{6} (4a^2 - L^2)}{6} \quad (20)$$

The equation for the frequency f_1 (cps) of the fundamental mode of vibration of a clamped circular diaphragm is given (Ref 7) by

$$f_1 = \frac{11.84 (144)}{8\pi} \frac{t}{a^2} \sqrt{\frac{g Y}{\gamma(1 - \nu^2)}} \quad (21)$$

where

- a = radius of diaphragm, in.,
- g = acceleration due to gravity, ft/sec²,
- γ = weight density, pcf,
- t = diaphragm thickness, in.,
- Y = Young's modulus, psi,
- ν = Poisson's ratio.

The equation for the deflection y_c (in.) at the center of a clamped diaphragm subjected to a uniform pressure is given (Ref 6) by

$$y_c = \frac{3 w a^4 (1 - \nu^2)}{16 Y t^3} \quad (22)$$

where

- w = pressure on diaphragm, psi,
- a = radius of diaphragm, in.,
- t = thickness of diaphragm, in.

The signs have been selected so that for positive pressure, the deflection will be positive in the direction produced by the pressure.

Equations (21) and (22) will be used to provide the design that will satisfy the natural frequency and stiffness specifications, respectively, for the gage.

4. PIEZORESISTIVE COMPRESSION ELEMENTS

In evaluating the possible applications of solid piezoresistive elements for measuring one component of compressive stress in soil, it is convenient to consider a crystal of this material in the form of a rectangular solid with one face perpendicular to the direction of this stress. The response of this piezoresistive element will be affected by the direction of current flow and the direction of voltage measurement (these need not be coincident), the crystal axis orientation, the normal and shear stresses acting on each face, and the piezoresistive coefficients. The first phase of analysis consists primarily of assessing the influence of each of these factors.

It was immediately determined that if an element were selected whose thickness in the direction of the desired stress was small compared with its other dimensions, i.e., commensurate with a disk configuration, then it would not be feasible to use this direction for the current or voltage because the circuit resistance would be too low with available piezoresistive materials. The remaining choices are for the current and voltage directions to be perpendicular to the measured stress direction. Further analysis shows that there is no advantage in making the current and voltage perpendicular to each other, hence the investigation may be restricted to those cases in which the current and voltage axes are coincident and perpendicular to the direction of normal stress to be measured.

The general case to be analyzed is illustrated in Figure 2. The stress on the element caused by the desired normal stress in the soil is T_2' . The current I and voltage E are taken in the $1'$ direction. The orthogonal coordinate system shown ($1'$, $2'$, $3'$)

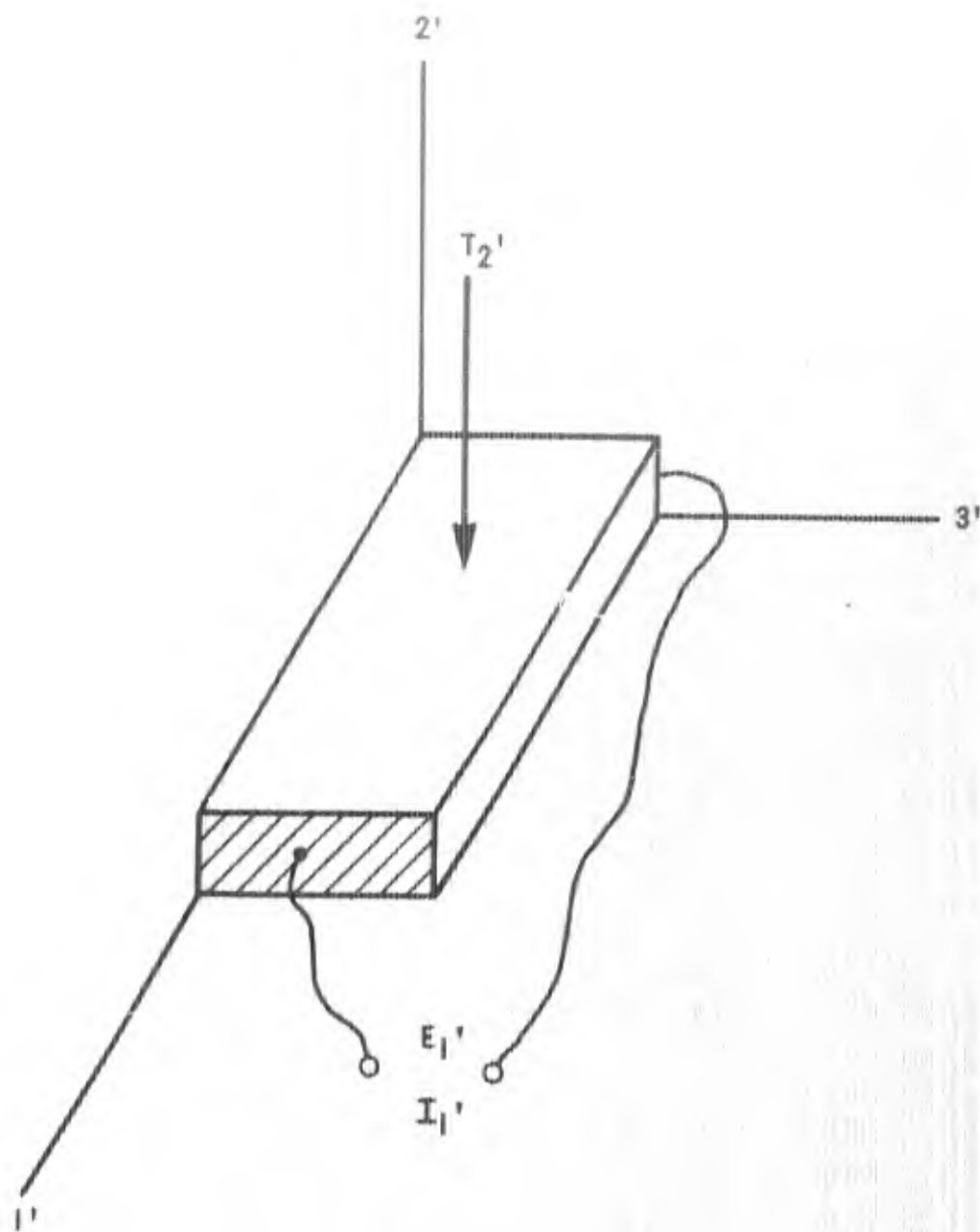


Figure 2. Transverse Element Configuration

is at an arbitrary orientation with respect to the crystal axes of the piezoresistive material. Other stresses may be present on the faces of the element.

Since $I_2' = I_3' = 0$, Eq (9) may be written as

$$E_1'/I_1' = \rho_0 \left(1 + \pi_{11}'T_1' + \pi_{12}'T_2' + \pi_{13}'T_3' + \pi_{14}'T_4' + \pi_{15}'T_5' + \pi_{16}'T_6' \right) \quad (23)$$

Assume a normal force, uniformly distributed, on one of the faces of the disk with negligible bending of the disk because of the applied force. If only the stress T_2' is present, then Eq (23) becomes

$$\begin{aligned} E_1'/I_1' &= \rho_0 \left(1 + \pi_{12}'T_2' \right) \\ &= \rho_0 + \Delta\rho \end{aligned} \quad (24)$$

where

$$\frac{\Delta\rho}{\rho_0} = \pi_{12}'T_2' \quad (25)$$

Equation (25) holds if the changes in resistance caused by changes in volume of the disk are negligible with respect to the change of resistance caused by the piezoresistive effect.

In terms of the piezoresistive constants of the crystal, Table I, page 12, gives

$$\pi_{12}' = \pi_{12} + \lambda \left(\pi_{11} - \pi_{12} - \pi_{44} \right) \quad (26)$$

where

$$\lambda = \left[\left(l_1 l_2 \right)^2 + \left(m_1 m_2 \right)^2 + \left(n_1 n_2 \right)^2 \right]^{-1/2}$$

For maximum change in resistivity, π_{12}' must be maximized. The expression for λ has extreme values of 0 and 1/2. The orientation of the crystal for $\lambda = 0$ is given by Eq (27).

$$\begin{bmatrix} l_1 & m_1 & n_1 \\ l_2 & m_2 & n_2 \\ l_3 & m_3 & n_3 \end{bmatrix} = \begin{bmatrix} 1 & 0 & 0 \\ 0 & \text{any} \\ 0 & \text{comparable} \\ & \text{direction} \end{bmatrix} \quad (27)$$

i.e., the 1 and 1' axes are coincident and 2' and 3' may have any rotation about 1'.

For $\lambda = 1/2$:

$$\begin{bmatrix} l_1 & m_1 & n_1 \\ l_2 & m_2 & n_2 \\ l_3 & m_3 & n_3 \end{bmatrix} = \begin{bmatrix} \frac{1}{\sqrt{2}} & \frac{1}{\sqrt{2}} & 0 \\ \frac{-1}{\sqrt{2}} & \frac{1}{\sqrt{2}} & 0 \\ 0 & 0 & 1 \end{bmatrix} \quad (28)$$

i.e., the 3 and 3' axes are coincident and the 1' and 2' axes are rotated about 3 such that the 1' axes is 45 deg from the 1 and 2 axes. Call the case of $\lambda = 0$, Case I, and $\lambda = 1/2$, Case II. For Case I

$$\pi_{12}' = \pi_{12} \quad (29)$$

while for Case II

$$\pi_{12}' = 1/2 \left(\pi_{12} + \pi_{11} - \pi_{44} \right) \quad (30)$$

Representative values of the piezoresistive coefficients for n- and p-type silicon and germanium are given in Table II.

Table II
PIEZORESISTIVE COEFFICIENTS

Material	ρ_0 (ohm-cm)	π_{11}	π_{12} cm ² /dyne	π_{44}
n-Silicon	11.7	-102.0×10^{-12}	53.4×10^{-12}	-13.6×10^{-12}
p-Silicon	7.8	7.5×10^{-12}	-1.0×10^{-12}	138.0×10^{-12}
n-Germanium	9.9	-4.7×10^{-12}	-5.0×10^{-12}	-138.0×10^{-12}
p-Germanium	15.0	-10.6×10^{-12}	5.0×10^{-12}	98.6×10^{-12}

For Case I, the only significant π_{12} coefficient is that of n-silicon. The optimum orientation for this case would be with the faces of the disk parallel to the crystal faces, giving $\pi_{12}' = 53.4$.

For Case II, π_{12}' for each of the four materials may be calculated from Eq (30). The results are shown in Table III.

Table III
TRANSVERSE PIEZORESISTIVE COEFFICIENT

Material	π_{12}' (cm ² /dyne)
n-Silicon	-17.5×10^{-12}
p-Silicon	-65.8×10^{-12}
n-Germanium	64.2×10^{-12}
p-Germanium	-52.1×10^{-12}

The orientation for Case II is such that the plane of the disk is (001) and the current is the [110] direction. According to Table III the maximum sensitivity is given if p-silicon is used, although n-germanium is essentially the same. If dimensional changes are neglected

$$\frac{\Delta R}{R_0} = \frac{\Delta \rho}{\rho_0} \quad (31)$$

Young's modulus is given by

$$Y = \frac{T}{\epsilon} \text{ dynes/cm}^2 \quad (32)$$

Using Eq (25), (31), and (32), Eq (11) becomes

$$K = \pi_{12}' Y \quad (33)$$

For p-silicon, Young's modulus is approximately 1.7×10^{12} dynes/cm² in the [111] direction. Inserting the appropriate

value from Table III into Eq (33), the gage factor can, therefore, be shown to be as large as -111.9 as compared to gage factors of from 2 to 5 for conventional wire and foil gages.

If a maximum load of 500 psi (3.45×10^7 dynes/cm²) is assumed evenly distributed over the face of the disk, the change in resistance of the disk may be calculated from Eq (11) and (32), and can be shown to be, for the case cited, approximately 0.23 percent. This change in resistance is independent of the size of the disk. Using Eq (11), (32), and (33) the change in resistance can be shown to be, in general, given by

$$\frac{\Delta R}{R_0} = \pi_{12}' T_2' . \quad (34)$$

Of interest in any gage design are the effects of transverse stresses upon the gage output. For the case where the total stress on the gage may be resolved into three normal stresses, T_1' , T_2' , and T_3' , Eq (23) reduces to

$$E_1'/I_1' = \rho_0 \left(1 + \pi_{11}' T_1' + \pi_{12}' T_2' + \pi_{13}' T_3' \right) . \quad (35)$$

The resistivity change is therefore the last three terms in parentheses or

$$\frac{\Delta \rho}{\rho_0} = \pi_{11}' T_1' + \pi_{12}' T_2' + \pi_{13}' T_3' . \quad (36)$$

For the case under consideration, the effect of T_1' and T_3' is to be minimized while maximizing the effect of T_2' . This can be accomplished by minimizing π_{11}' and π_{13}' while maximizing π_{12}' . The primed piezoresistive coefficients were given in Table I, page 12 .

Substituting Eq (27) and (28) into the appropriate expressions gives for Case I:

$$\begin{aligned} \pi_{11}' &= \pi_{11} , \\ \pi_{13}' &= \pi_{12} , \\ \pi_{12}' &= \pi_{12} . \end{aligned} \quad (37)$$

Since π_{12}' is equal to π_{13}' and π_{11}' is greater than or equal to π_{12}' the effects of the lateral stresses cannot be minimized by selecting the crystal axis orientation as in Case I.

Similarly for Case II

$$\pi_{11}' = 1/2 \left(\pi_{11} + \pi_{12} + \pi_{44} \right),$$

$$\pi_{13}' = \pi_{12}, \quad (38)$$

$$\pi_{12}' = 1/2 \left(\pi_{11} + \pi_{12} - \pi_{44} \right).$$

In this case, it is necessary to examine the magnitude of each of these coefficients for all of the four materials which are available, namely, n- and p- type silicon and germanium. Table IV gives the value of the prime coefficient for each of these materials. It can be seen that in no case is π_{12}' significantly greater than each of the other two coefficients. Once again, this indicates that the effect of an unwanted stress is approximately equal to that which it is desired to measure. Therefore, the effect of the unwanted stresses must be eliminated from the element mechanically rather than electrically.

Table IV
PIEZORESISTIVE COEFFICIENTS

Material	π_{11}'	π_{13}' (cm^2/dyne)	π_{12}'
n-Silicon	-31.1×10^{-12}	53.4×10^{-12}	-17.5×10^{-12}
p-Silicon	72.3×10^{-12}	-1.0×10^{-12}	-65.8×10^{-12}
n-Germanium	-73.9×10^{-12}	-5.0×10^{-12}	$+64.2 \times 10^{-12}$
p-Germanium	46.5×10^{-12}	5.0×10^{-12}	-52.1×10^{-12}

It is also of interest to consider the effects of shear stresses on the output of the gage. For the case under consideration, that is, the current and voltage in the 1' direction, shear stresses will affect the output by the π_{16}' , π_{15}' , and π_{14}' coefficients (Eq (23)). In Case I, since l_1 is equal to 1, l_2 and l_3 must be zero for a cubic crystal. In addition, m_1 and n_1 are zero. Therefore, for Case I, all three piezoresistive shear stress coefficients vanish. For Case II, l_3, m_3, n_1 , and n_2 are zero. Therefore, once again the three shear stress piezoresistive coefficients vanish. Hence, in both cases, shear stresses will have no effect on the output on the thin disk element.

The resistive change of a single strain gage element is usually determined by means of a bridge circuit of which the strain gage is one arm. For a p-silicon strain gage, the change in resistance for a stress of 500 psi has been previously shown to be approximately 0.23 percent. If used in a bridge in which only one arm is active, the output voltage will be 0.576 mv/volt applied. If two such gages are used as opposite arms of the bridge, the output of the bridge will be doubled.

The maximum sensitivity would be obtained if two additional bridge arms were used whose resistance changed in the opposite sense to the p-silicon strain gages. This condition could be obtained if n-silicon were used for the two additional active arms. For the n-type material, the change in resistance under stress is approximately two-thirds of that obtained with the p-type material. For this case, the bridge output can be shown to be more than three times that which is obtained when only a single sensing element is used. The output voltage would be about 2 mv/volt applied.

5. PIEZORESISTIVE BENDING ELEMENT

A cantilever beam arrangement may also be considered as a possible application of piezoresistive elements. The configuration of such a element is shown in Figure 3. Current in the 1' direction only is assumed. The ratio of the voltage to the current in the 1' direction is given on page 31.

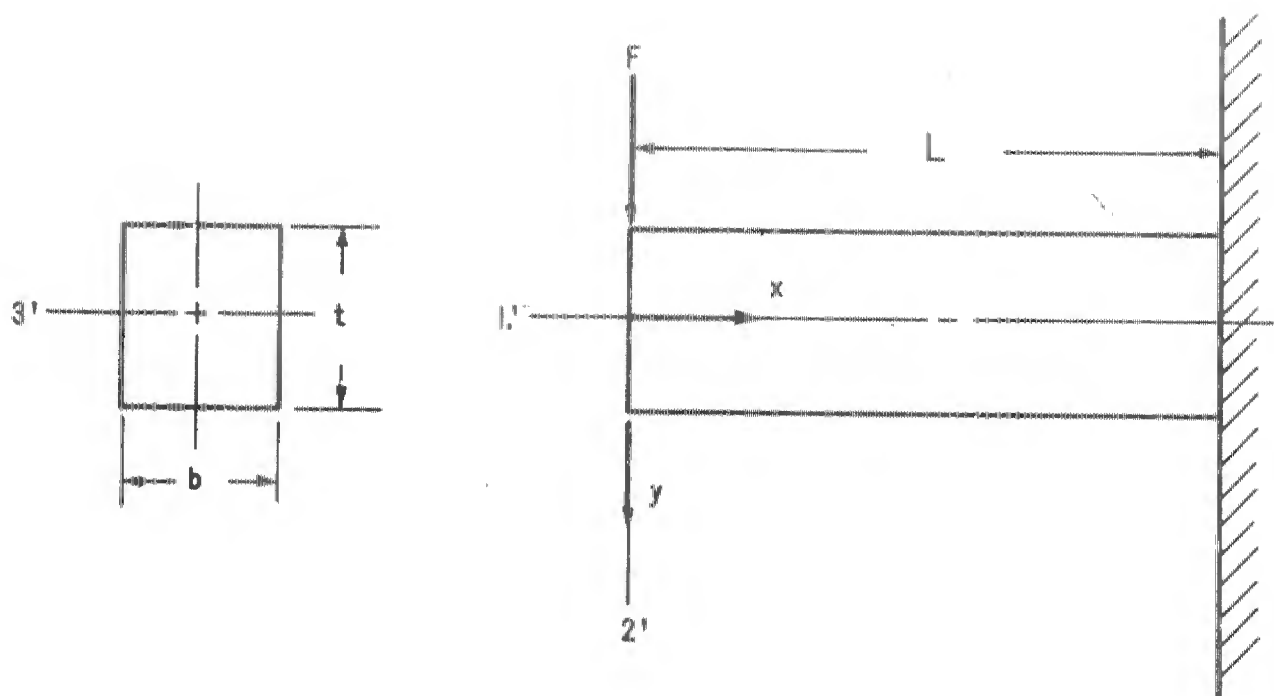


Figure 3. Cantilever Beam Gage

The ratio of the voltage to the current in the 1' direction is given by

$$E_1' / I_1' = \rho_0 \left(1 + \pi_{11}' T_1' + \pi_{16}' T_6' \right), \quad (39)$$

which gives

$$\frac{\Delta \rho}{\rho_0} = \pi_{11}' T_1' + \pi_{16}' T_6'. \quad (40)$$

Table I, page 12, gives π_{11}' and π_{16}' in terms of the piezoresistive coefficients of the crystal and the direction cosines between the crystal axes and the arbitrary primed axes selected. Consider the magnitude of the piezoresistive coefficients for the orientations used with the thin disk. For Case I, π_{11}' is equal to π_{11} while π_{16}' is equal to zero. Thus, the output will be independent of the shear stress; it will only depend upon the tension or compression of the beam. The maximum value of π_{11} from Table II, page 25, is found to be that of n-silicon. The beam such as shown might be fabricated by electrically isolating the upper and lower halves of the beam, using the same materials for each half. Since the upper half of the beam is in tension, and the lower half is in compression, the two halves of the beam would change resistance in opposite directions. Each half could be used as one arm of a bridge. The entire beam would then constitute two arms of a bridge.

For Case II, π_{11}' is nonzero while π_{16}' vanishes so that for this case also the beam will not respond to the shear stress. The coefficient π_{11}' in this case will again be given by Eq (38) and its magnitude will be the same as given in Table III, page 26.

Case I corresponds to aligning the crystal so that the loading is parallel to one of the crystal axes. For this case, the maximum effect occurs in n-type silicon. For each of the other three semiconductor materials, the maximum longitudinal coefficient π_{11}' occurs along a [111] direction. It is, therefore, of interest to determine the magnitude of this coefficient for this latter orientation and also the magnitude of the shear stress coefficient.

For the case of the l' axis oriented in the $[111]$ direction of the crystal, the direction cosines for this transformation are given by

$$\begin{bmatrix} l_1 & m_1 & n_1 \\ l_2 & m_2 & n_2 \\ l_3 & m_3 & n_3 \end{bmatrix} = \begin{bmatrix} \frac{1}{\sqrt{3}} & \frac{1}{\sqrt{3}} & \frac{1}{\sqrt{3}} \\ -\frac{1}{\sqrt{3}} & \frac{1}{\sqrt{3}} & -\frac{1}{\sqrt{3}} \\ -\frac{1}{\sqrt{3}} & -\frac{1}{\sqrt{3}} & \frac{1}{\sqrt{3}} \end{bmatrix} . \quad (41)$$

If these direction cosines are substituted into the expression for π_{16}' , it is found that this coefficient does not vanish, but is equal to

$$\pi_{16}' = -\frac{2}{9} \left(\pi_{11} - \pi_{12} - \pi_{44} \right) . \quad (42)$$

The magnitude of this coefficient can be appreciable. The total effect which the shear stress would have upon the output would depend upon the relative magnitude of the shear stress as compared to the longitudinal stress. For n-type germanium and p-type silicon, the magnitude of the shear stress piezoresistive coefficient is approximately one-half of the longitudinal coefficient while in p-type germanium the magnitude of π_{16}' is greater than the longitudinal piezoresistive coefficient.

The normal stress varies linearly with the distance from the end of the beam and the distance from the neutral axis. First consider only a simple case where the semiconducting material is a thin layer on both sides of a thicker substrate. A side view of the beam is given in Figure 4. For this case, the stress across the thickness of the film can be assumed constant. The variation of the stress will then be along the length of the beam. The unstressed resistance of either layer is given by Eq (15). The resistivity along the length of the beam is given by

$$\begin{aligned} \rho &= \rho_0 + \Delta\rho \\ &= \rho_0 \left(1 + \frac{\Delta\rho}{\rho_0} \right) , \end{aligned} \quad (43)$$

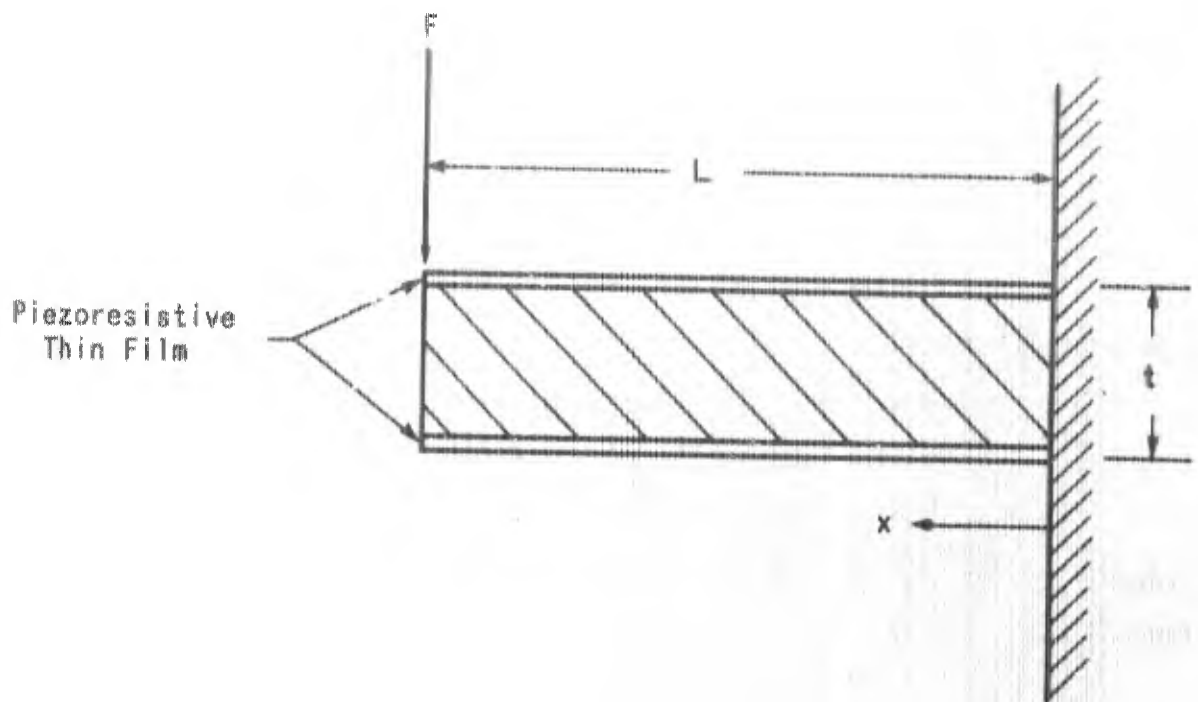


Figure 4. Thin Film Cantilever Gage

but

$$\frac{\Delta \rho}{\rho_0} = \pi_{11} 'T_1' \quad , \quad (44)$$

therefore,

$$\rho = \rho_0 \left(1 + \pi_{11} 'T_1' \right) \quad . \quad (45)$$

The stress is a linear function of the distance from the support being zero at the free end of the beam and maximum at the fixed end. The stress is given by

$$T = T_{\max} \left(1 - \frac{x}{L} \right) \quad . \quad (46)$$

Then

$$\rho = \rho_0 \left[1 + \pi_{11} 'T_{\max} \left(1 - \frac{x}{L} \right) \right] \quad . \quad (47)$$

The total resistance is given by

$$R_T = \frac{1}{A} \int_0^L \rho(x) dx \quad . \quad (48)$$

Substituting Eq (47) into Eq (48) and integrating, gives the total resistance

$$R_T = \frac{\rho_0 L}{A} \left(1 + \frac{1}{2} \pi_{11} 'T_{\max} \right) \quad . \quad (49)$$

The change in resistance is, therefore, given by

$$\frac{\Delta R}{R_0} = \frac{1}{2} \pi_{11} 'T_{\max} \quad . \quad (50)$$

For a cantilever beam

$$T_{\max} = \frac{6FL}{bt^2} \quad , \quad (51)$$

where

F = applied force,
 L = length of beam,
 t = thickness of the beam,
 b = width of the beam.

In terms of the dimensions of the beam and the applied force, the maximum stress is, therefore, given by

$$T_{\max} = 6 \frac{FL}{bt^2} \quad (52)$$

from which

$$\frac{\Delta R}{R_0} = 3 \pi_{11} \frac{FL}{bt^2} \quad (53)$$

The exact value of $\Delta R/R_0$ would depend upon the gage design. The fracture stress of silicon and germanium is about 3×10^9 dynes/cm². This limiting stress would also have to be taken into consideration in the design of a practical gage.

For the case where the entire beam is piezoresistive, the analysis becomes more complicated. The stress in the beam shown in Figure 3 will be a function of both the x and y positions, and resistivity is a function of the stress, hence

$$\rho = f(x, y) \quad (54)$$

The resistance of the upper or lower half of the beam will, therefore, require a double integration and will be given, for the upper half of the beam, by

$$R_u = \frac{1}{b} \int_0^L \frac{dx}{\int_0^{t/2} \frac{dy}{\rho(x, y)}} \quad (55)$$

The integral in the denominator represents parallel summation of the resistance of length dx and thickness dy over the half thickness of the beam. The integral in the numerator then represents series summation of the resulting elements of thickness dy and lateral dimensions b by $t/2$ over the length of the beam.

The resistivity is given by Eq (45) in which T_1' is given by

$$T_1' = \left(\frac{12F}{bt^3} \right) xy, \quad (56)$$

where

x = distance from the free end of the beam

y = distance from the neutral axis.

Substituting Eq (56) into Eq (45) and the result into Eq (55) gives

$$R_u = \frac{1}{b} \int_0^L \frac{dx}{\int_0^{t/2} \frac{dy}{\rho_0 \left(1 - \frac{12F}{bt^3} \pi_{11}' xy \right)}} \quad (57)$$

Carrying out the integration with respect to y gives

$$R_u = - \frac{F \pi_{11}' \rho_0}{bI} \int_0^L \frac{x dx}{\ln \left(1 - \frac{6F \pi_{11}' tx}{bt^3} \right)}. \quad (58)$$

The result of this integration is an infinite series and is given by

$$R_u = \frac{\rho_0 t}{3F \pi_{11}'} \sum_{n=1}^{\infty} \frac{(2^n - 1) \left[\ln \left(1 - \frac{6F \pi_{11}' L}{bt^2} \right) \right]^n}{n \cdot n!}. \quad (59)$$

The resistance given by Eq (59) is that of the upper half of the beam. For the lower half of the beam, which is in compression, an analogous expression can be derived. This resistance is

$$R_L = \frac{\rho_0 t}{3F \pi_{11}'} \sum_{n=1}^{\infty} \frac{(2^n - 1) \left[\ln \left(1 + \frac{6F \pi_{11}' L}{bt^2} \right) \right]^n}{n \cdot n!}. \quad (60)$$

In either case, the resistance is of the form

$$R = J \left\{ \ln(1 + \alpha) + \frac{3}{2} \frac{\alpha^2}{2!} \left[\ln(1 + \alpha) \right]^2 + \dots \right\}, \quad (61)$$

where

$$J = \frac{\rho_o L}{3F \pi_{11}'},$$

and

$$\alpha = \pm \frac{6F \pi_{11}' L}{bt^2}.$$

If $|\alpha| < 1$ the logarithmic terms may be expanded in a power series in α . Neglecting all but the first and second order terms gives

$$R \approx J \left(\alpha + \frac{1}{4} \alpha^2 \right), \quad (62)$$

which may be written as

$$R \approx - \frac{2 \rho_o L}{bt} \left(1 \pm \frac{6F \pi_{11}' L}{4bt^2} \right). \quad (63)$$

This is of the form

$$R = R_o \left(1 \mp \frac{\Delta R}{R_o} \right). \quad (64)$$

Therefore,

$$\frac{\Delta R}{R_o} = \pm \frac{3}{2} \pi_{11}' \left(\frac{FL}{bt^2} \right). \quad (65)$$

The approximation given by Eq (65) is in error by less than 1.5 per cent for values of α of up to 0.5. A comparison of Eq (65) with Eq (53) shows that for the same size beam element and loading the sensitivity is halved by making the entire beam out of the piezoresistive material. This situation occurs because the material in the entire beam is stressed at an average of one half the level of the material at the outer surfaces and because the cross-sectional area does not influence the $\Delta R/R$ term.

6. OTHER PIEZORESISTIVE GAGE DEVELOPMENTS

At the beginning of this study an inquiry was made to determine what other organizations might have developed or might be developing soil stress gages using piezoresistive transducers. Three organizations were found to be experimenting with gages involving semiconductor strain elements:

1. Eric H. Wang Civil Engineering Research Facility (formerly called Air Force Shock Tube Laboratory), Albuquerque, New Mexico, operated by the University of New Mexico (UNM).
2. Nuclear Weapons Effects Division, U. S. Army Engineer Waterways Experiment Station (WES), Vicksburg, Mississippi (Ref 8).
3. Department of Civil Engineering, Columbia University, New York, New York (Ref 9).

The UNM gage is illustrated in Figure 5. The exact details of the gage construction were not available, but the essential features are represented. The gage was designed for a stress range of 0 to 1500 psi. Its sensing element is a solid column isolated from lateral pressures by an air gap. Two semiconductor strain gages are aligned vertically on the outside of the column. Each gage has a p- and n-silicon element so that a full bridge can be obtained by measuring only the vertical strain in the column when the column is subjected to soil pressures on the exposed end. The gage is extremely stiff and has a thickness-diameter ratio of 1.33. It was hoped that by making the sensing area only a portion of the total area (approximately 30 percent) separated by a gap, that the tendency for overregistration of the gage in soil would be reduced or eliminated.

The WES and Columbia University gages were similar in concept. Both utilized piezoresistive strain gages mounted on a stiff diaphragm that was in contact with the soil. These gages are illustrated in Figures 6 and 7.

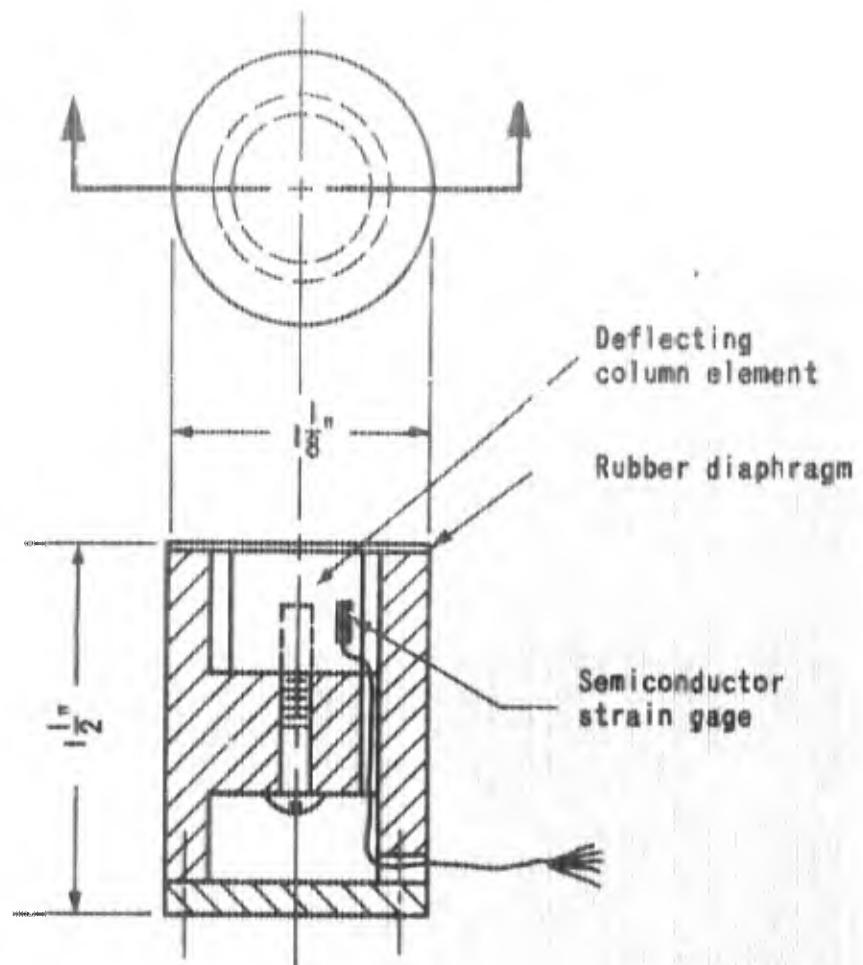


Figure 5. Schematic of UNM Soil Stress Gage

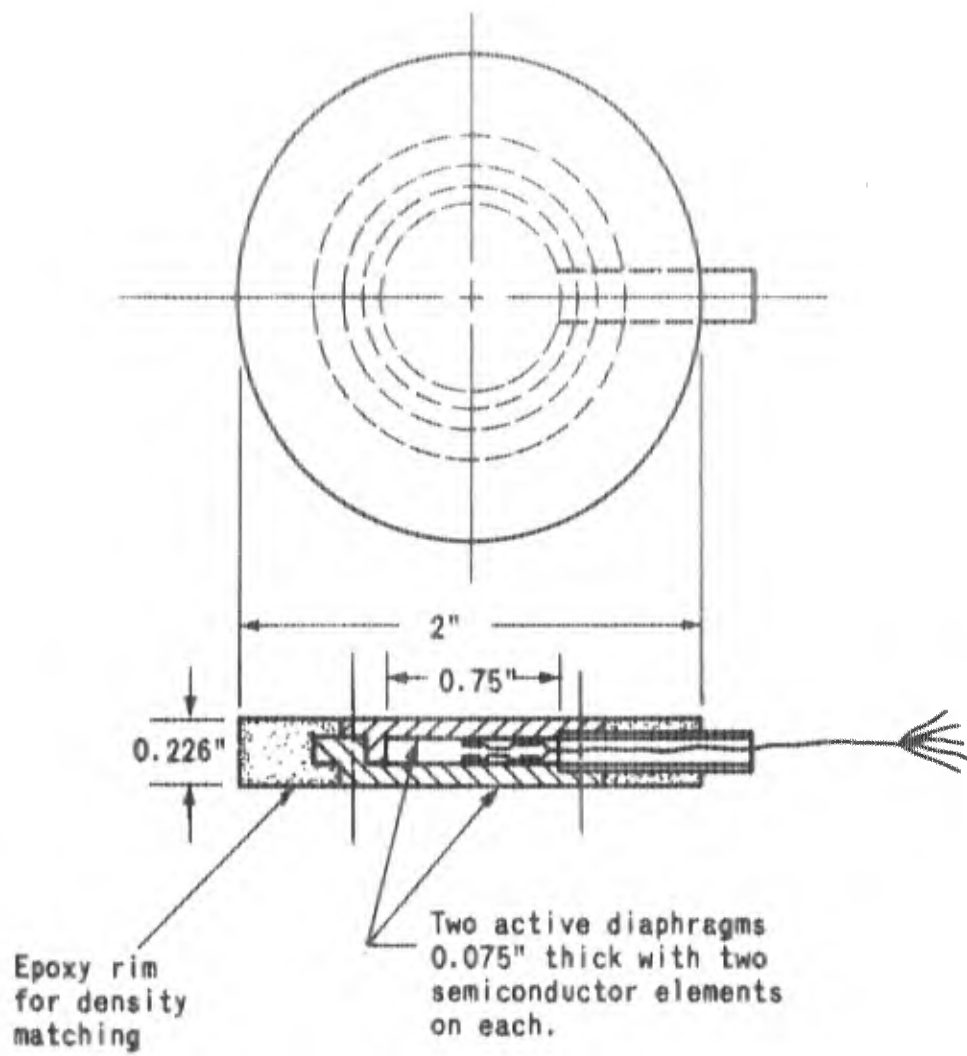


Figure 6. Schematic of WES Soil Stress Gage

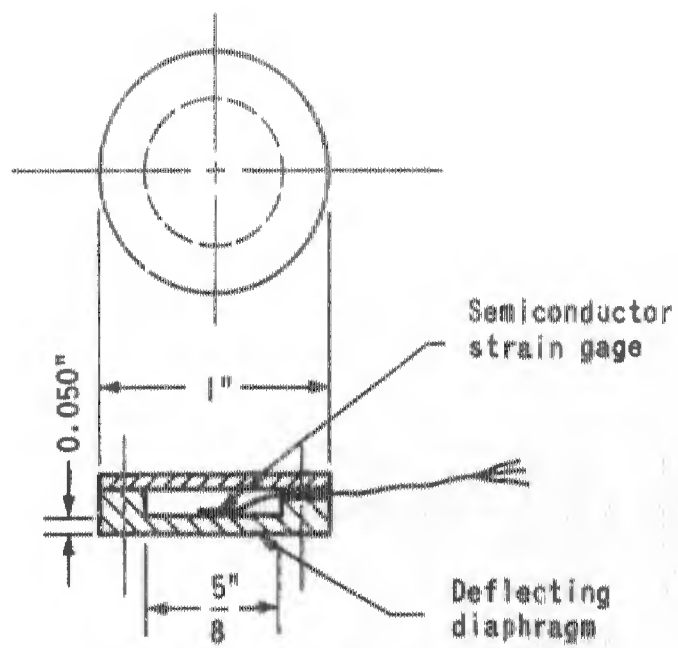


Figure 7. Schematic of Columbia University Soil Stress Gage

The WES gage (Figure 6) has two active diaphragms of equal stiffness. A full bridge is obtained by placing the semiconductor elements both in the center and at the edge of each diaphragm. The diaphragms are machined from stainless steel. An epoxy rim is added to match the bulk density of the gage to that of the soil and to provide the required thickness-diameter ratio. A specially constructed hermetic feed-through is used to isolate the gage interior from pore pressures in the soil.

The thickness-diameter ratio of this gage is 0.113, the bulk density is 100 pcf, the diameter-deflection ratio of each diaphragm at 500 psi is estimated to be around 5600, the natural frequency of the diaphragm is 40,000 cps and the design pressure range is 0 to 500 psi.

An evaluation of the sensitivity of the WES gage to acceleration was made by mounting it on a drop table. These tests showed that for levels up to about 90 g the acceleration sensitivity was extremely small, approximately 0.04 psi/g. In spite of the full bridge circuit the gage was still found to be fairly temperature sensitive (approximately 1 psi/°F). This is not considered to be a serious limitation for most soil applications, however. Tests in soil indicated that the gage overregistered by 10 to 30 percent.

The Columbia University gage has a thickness-diameter ratio of about 0.25 and the natural frequency is estimated to be 15,000 cps. The stress range for which the gage was designed was apparently about 0 to 100 psi. The gage had only one active diaphragm. A pair of p- and n-silicon semiconductor strain elements were used to provide a temperature compensated half-bridge circuit. The gages were calibrated in soil under static stress and these calibrations used to predict the stresses produced by subsequent dynamic loading.

SECTION V

GAGE DEVELOPMENT

All of the concepts analyzed in Section IV are theoretically feasible. In order to assess the practical advantages and limitations of each approach, including problems in fabrication, gages embodying each concept were designed and constructed for testing under hydrostatic pressure and in soil. The gage specifications on page 16 were used as a guide during this development phase, although these criteria were not always adhered to when they did not have a material effect on evaluation of the basic concepts.

It was determined from correspondence with manufacturers of piezoresistive materials that considerable effort would be required to obtain the necessary compression and bending elements for two of the gage concepts. These elements were not available as off-the-shelf items and there remained many problems in fabrication of the sensing elements. Therefore initial efforts were devoted to the diaphragm while the problems with the other transducers were being resolved.

1. CALIBRATION METHODS

Two methods of calibration were used for experimental evaluation of the stress gages. One provided a uniform hydrostatic pressure across both faces of the gage. The other provided a uniform stress field in confined samples of sand.

The apparatus for hydrostatic calibration is shown in Figure 8. The gage was mounted inside a spacer ring of identical thickness so that the gage would be free floating between two rubber diaphragms. The two chambers were filled with water at room temperature to provide a constant temperature environment. Air pressure from zero to 500 psi was applied to the water in both chambers simultaneously.

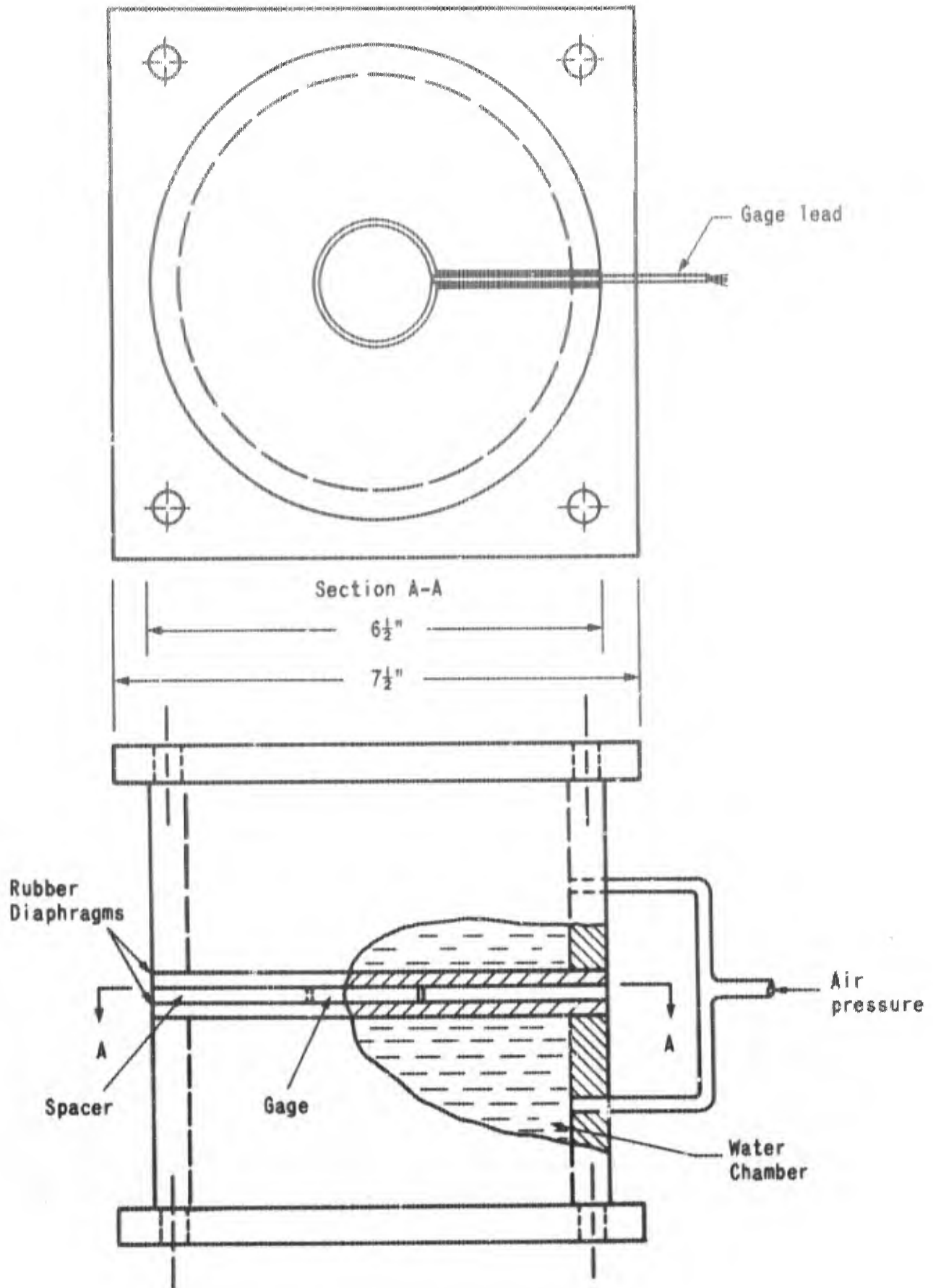


Figure 8. Hydrostatic Calibration Apparatus

The soil calibration chamber is illustrated in Figure 9. It is a pressure vessel 16 in. in diameter by 36 in. deep with 3 in. thick flat plates on each end. Air pressure up to 500 psi was applied through a rubber membrane to the soil surface, which was flush with the top of the vessel. The gages were placed at a depth of 3 to 4 in. and sufficiently far from the sides of the vessel to avoid the influence of friction between the soil and the walls. Only dry sand was used in these tests. The sand filling the bottom 30 in. of the vessel was vibrated to make it as dense as possible and minimize consolidation under pressure. Additional sand was added by raining techniques to the depth corresponding to that at which the gages were to be placed. The gages were then seated by pressing them carefully into the sand. The remaining sand was added and made flush with the top of the vessel.

A hypothetical response curve is shown in Figure 10. The parameters used to characterize this curve are illustrated. The nominal modulus or calibration constant is defined as the ratio of output voltage change from zero to the maximum applied pressure divided by this pressure change when one volt is applied to the bridge. Additional moduli were defined as the slope of the line between zero and the measured output at three-fourths of the maximum pressure. These values are approximately representative of the average modulus over the entire range of pressure. The nonlinearity during loading and unloading is expressed as the ratio in percent of the maximum deviation of voltage over the full range in pressure. The hysteresis is represented as a ratio in percent of the maximum voltage deviation between the loading and unloading curves to the total change in voltage over the full range in pressure.

2. DIAPHRAGM GAGE

Although concurrent efforts were underway by other investigators with the deflecting diaphragm gage discussed in Section IV, samples of these gages were not available for evaluation by IITRI.

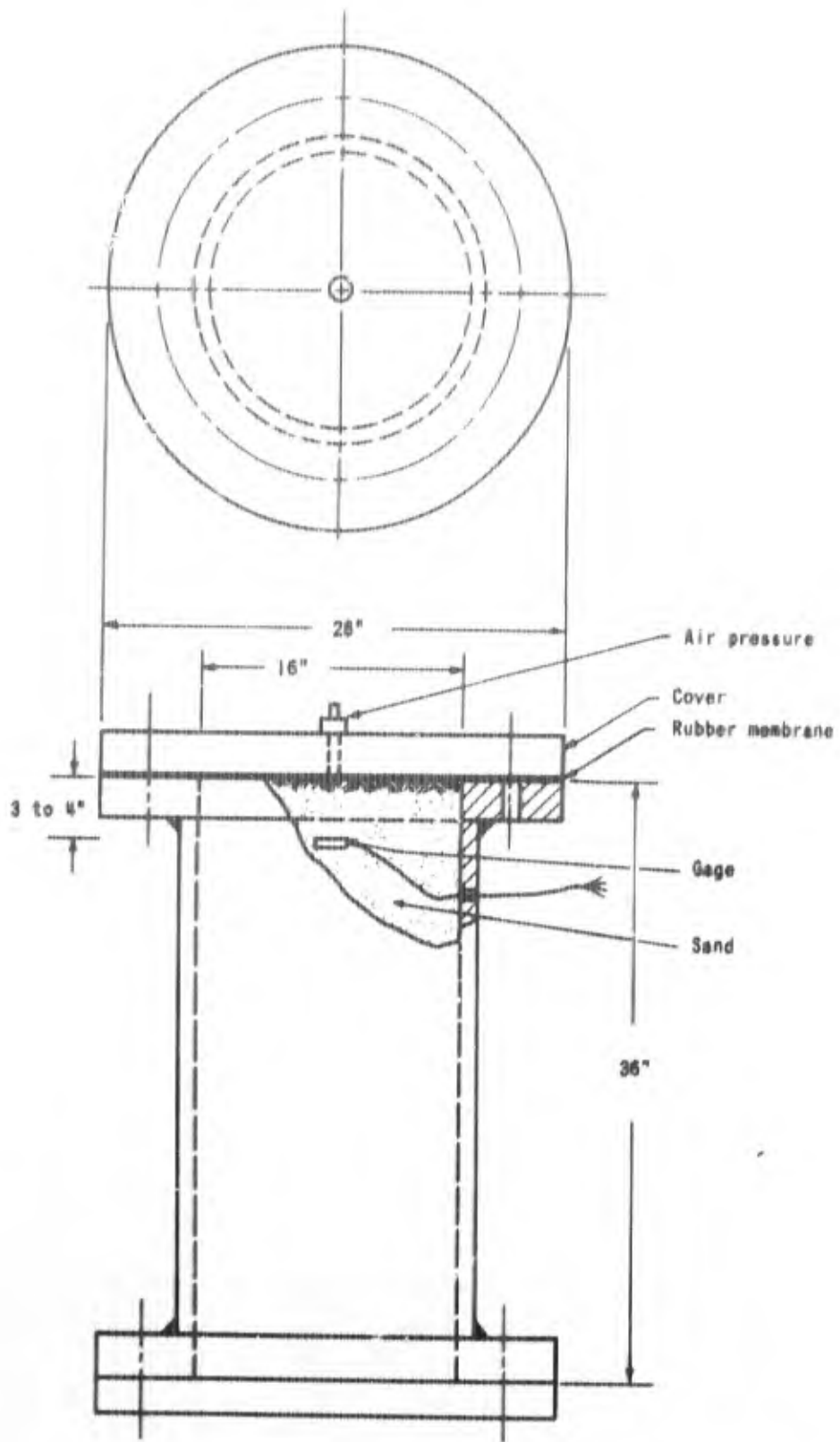


Figure 9. Soil Calibration Apparatus

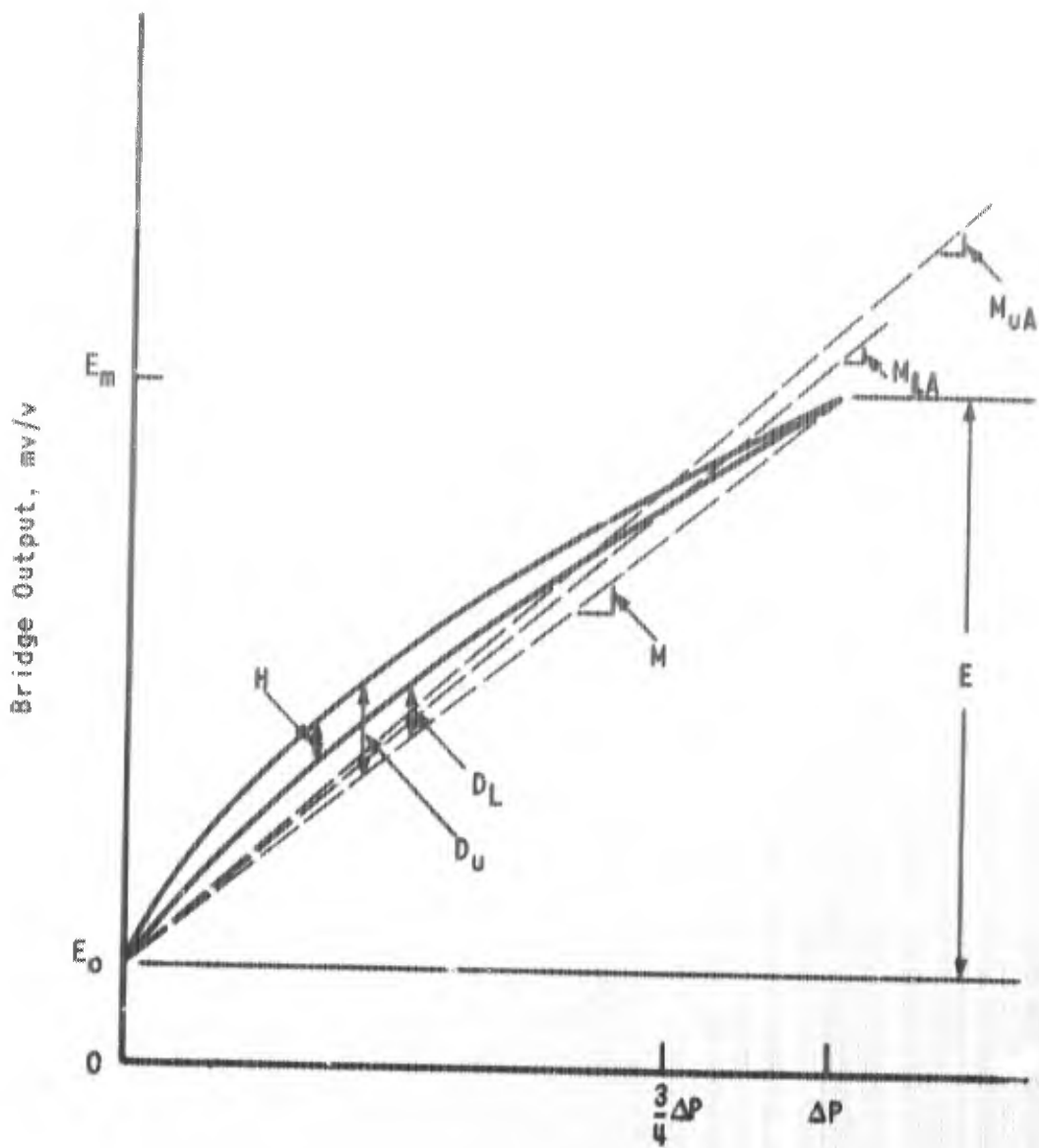


Figure 10. Characteristic Gage Response Curve

This concept was believed to have sufficient promise that its evaluation was considered an essential part of this study.

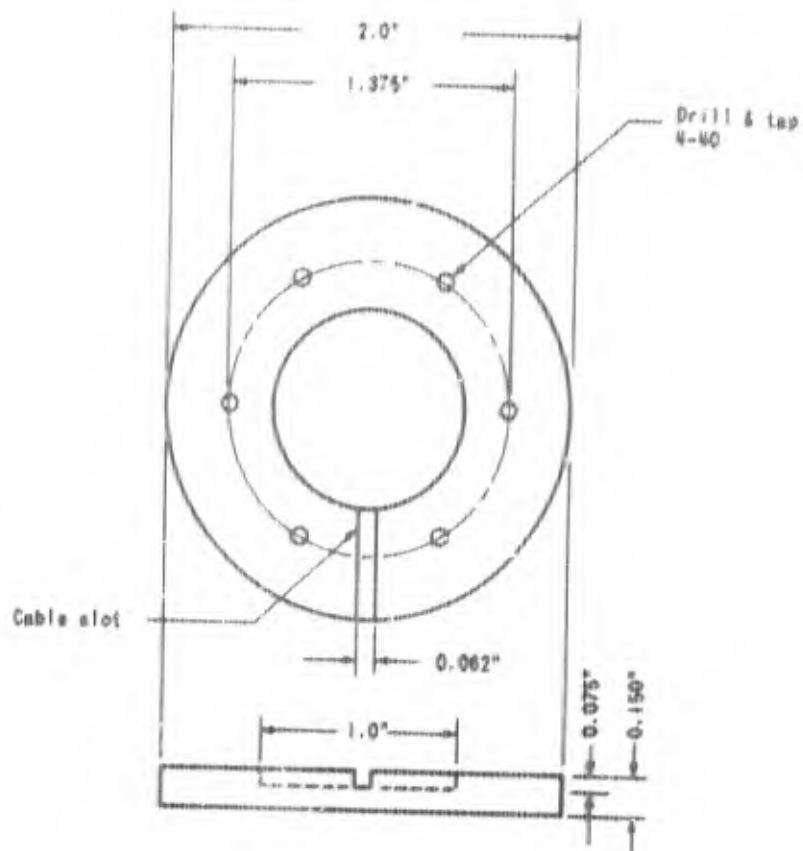
A diaphragm gage is the least complicated of the several gage types that are being considered for use in the measurement of soil stress. During the period when gage design concepts were being considered, information concerning the WES diaphragm gage was received including its dimensions and performance characteristics. Since IITRI concurred with the design criteria used for the WES gage it was decided to initially fabricate a gage having the same basic dimensions.

The first gage designed is illustrated in Figure 11 except that the inside case diameter was 0.75 in. It consists of two parts, a body and a cover, both machined from type 416 stainless steel. The hollowed interior of the body is 0.75 in. in diameter and 0.075 in. deep. When the gage is assembled, deflecting diaphragms 0.75 in. in diameter and 0.075 in. thick are provided in the center of each face. The overall gage diameter is 2 in. and the overall thickness is 0.225 in. Four-conductor shielded cable* was used with this and the other gages fabricated in this study. The overall diameter of the cable is 0.11 in. A slot was cut in the body of the gage to receive the cable. Since initial stages of evaluation were to be made in dry sand under static load, no attempt was made to waterproof the gage or to match its density to that of the soil. These criteria were to be met in the final design, however.

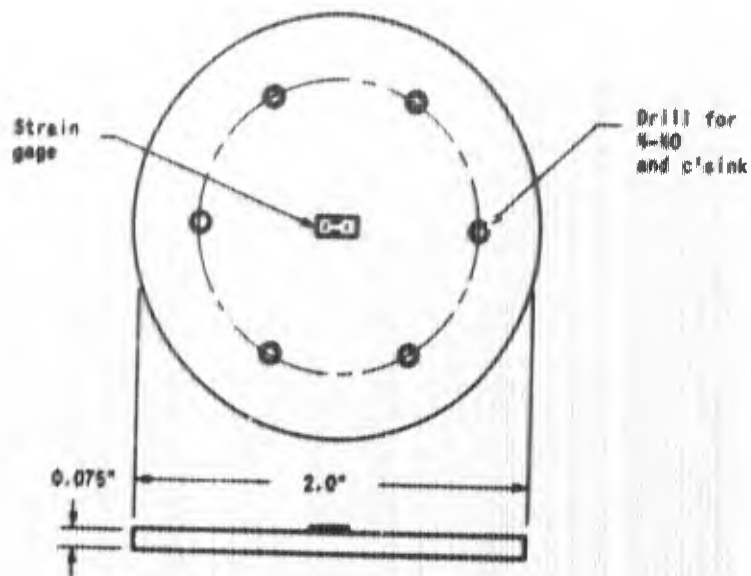
A four-arm diffused silicon strain gage** (Figure 12) was used with this first gage. The strain gage was 0.060 in. long by 0.020 in. wide. The manufacturer's literature indicated that it was designed for use with deflecting diaphragms. The nominal gage factor was 120 with each arm having a resistance of 1000 ohms. It seemed to be a logical choice for providing a full balanced

* Endevco Model 2920-33 shielded cable.

** Micro Systems Inc. Type SP4.



a) Case (Stainless Steel)



b) Cover (Stainless Steel)

Figure 11. Diaphragm Gage - Model I

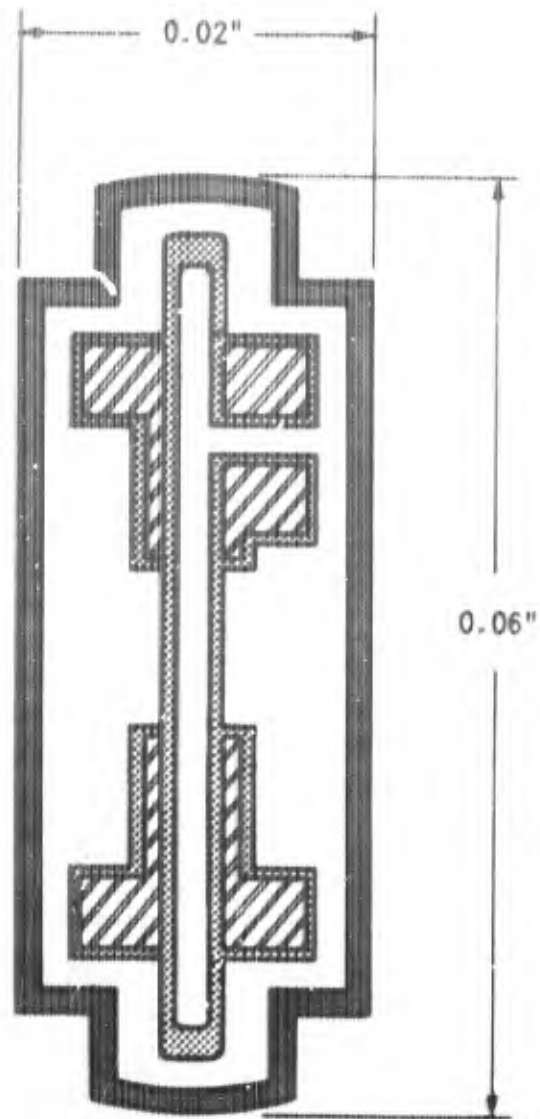


Figure 12. Four-Arm Diffused Silicon Strain Gage

bridge with complete temperature compensation. The strain gage was mounted with epoxy at the center of the cover diaphragm. This provides only one active diaphragm, a situation which may have some advantages near boundaries in the soil. The strain gage could have been placed on the body instead of the cover, but for the preliminary investigation the cover was more convenient.

Initial tests with this gage showed that the sensitivity was much lower than expected and not satisfactory. Also unexpectedly there was a large initial bridge unbalance and the gage appeared to be quite temperature sensitive. It was subsequently determined that the arms of the bridge were considerably different in resistance after the strain gage was mounted on the diaphragm.

In order to improve sensitivity the diameter of the recess in the gage body was increased from 0.75 in. to 1.0 in. (Figure 11). The physical characteristics of this gage, designated Model I, are listed in Table V. The gage thickness-diameter ratio is 0.112, the ratio of sensing area to total area is 0.25, the density is 450 pcf, and the diaphragm diameter-deflection ratio is 2370. The latter was reduced from 5600 when the diaphragm was increased in diameter from 0.75 to 1.0 in.

The hydrostatic calibration of the gage with this modification is shown in Figure 13. There is a large initial unbalance because of the change in resistance of the arms during mounting of the strain gage. There was no hysteresis in the load cycle from zero to 500 psi and back to zero again and the curve was repeatable; however, there was 3.6 percent nonlinearity. The calibration values are given in Table VI.

One of the four bridge arms was found to be significantly out of balance with the other three arms. This arm was disconnected and replaced with a fixed balancing resistor, leaving three active arms. The sensitivity was greatly improved (Figure 14, Table VI). The nonlinearity was essentially unchanged, however.

Table V
PHYSICAL CHARACTERISTICS OF GAGES TESTED

Model Designation	Overall Gage						Diaphragm					Characteristic Ratios				Transducers
	Diameter (in.)	Thickness (in.)	Density (pcf)	Material	Number of Active Arms	Nominal Sensitivity (mv/v/psi)	Diameter (in.)	Thickness (in.)	Center Strain (μ in./in.)	Center Deflection at 500 psi (10^{-4} in.)	Natural Frequency (kcps)	Gage Thickness + Diameter	Diaphragm Diameter + Deflection	Diaphragm Area + Gage Area	Diaphragm Deflection + Gage Thickness	
I	2	0.225	450	Stainless Steel	4	0.0137	1.0	0.075	252	4.22	30	0.112	2370	0.25	0.0187	Strain gage on diaphragm
IA	2	0.225	460	Stainless Steel	4	0.0154	0.75	0.075	141	1.34	53	0.112	5600	0.14	0.0060	Strain gages on diaphragm
IB	1.5	0.225	152	Aluminum	2	0.0378	0.75	0.10	240	1.67	71	0.15	4500	0.25	0.0074	Strain gage on diaphragm
II	2.0	0.225	470	Stainless Steel	2	-	0.75	0.075	-	< 1.34	-	0.112	> 5600	0.14	< 0.0060	Silicon in direct compression
III	2.0	0.232	485	Stainless Steel	3	0.0158	0.75	0.046	-	-	-	0.116	-	0.14	-	Strain gages on beam
UNM	1.125	1.5	91	Aluminum	4	0.0250	0.625	NA	NA	-	-	1.33	> 5600	0.31	< 0.0060	Strain gages on column

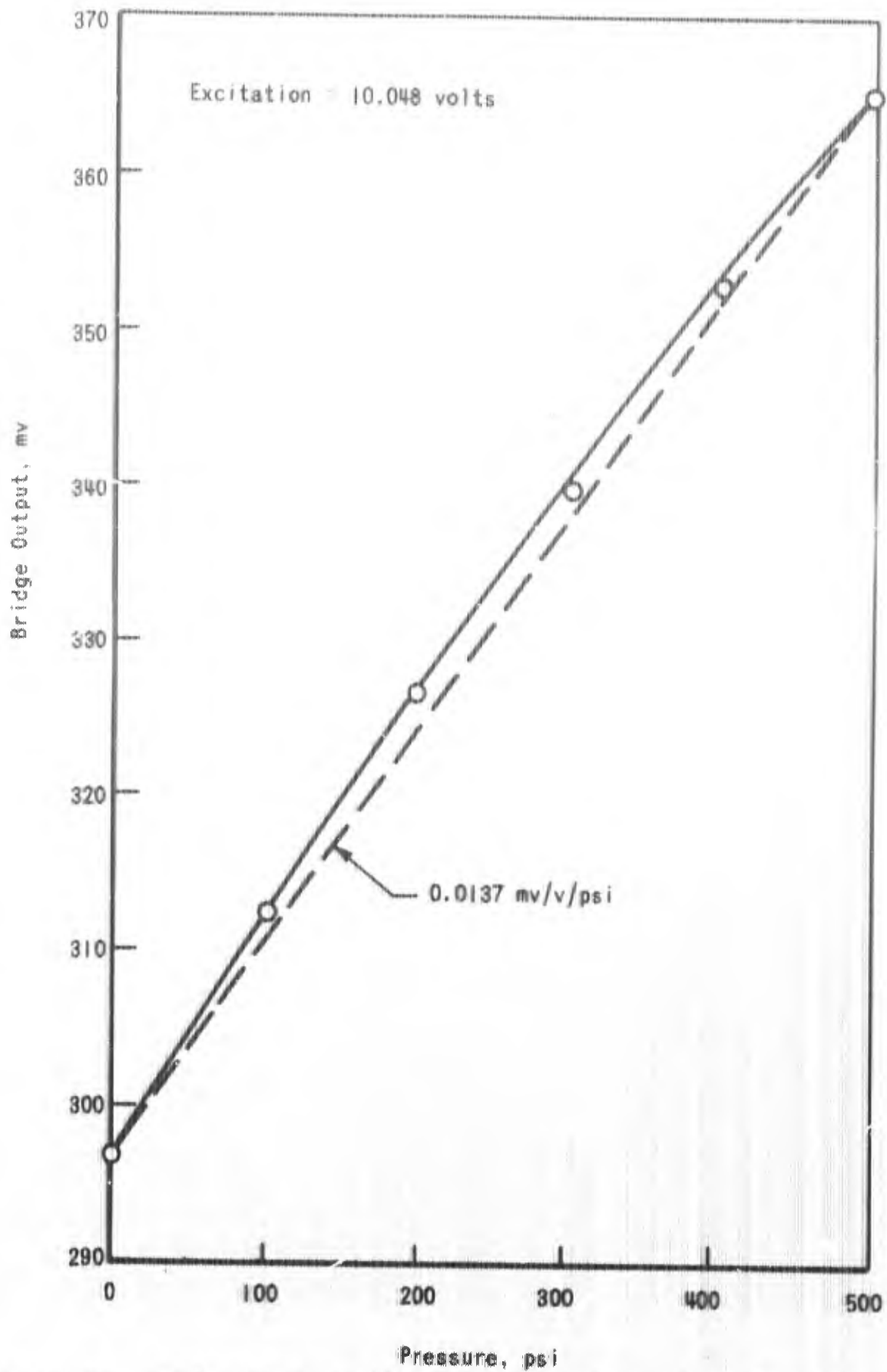


Figure 13. Hydrostatic Calibration of Model I Diagram Gage with Four Active Arms

Table VI
REPRESENTATIVE GAGE CALIBRATION DATA

Model Designation	Figure Number	Type of Test	Calibration Number	Cycle Number	Pressure Range (psi)	Nominal Modulus M(mv/v/psi)	Secant Modulus Load (mv/v/psi)	Secant Modulus Unload (mv/v/psi)	Nonlinearity Load D_L/E_L (%)	Nonlinearity Unload D_U/E_U (%)	Hysteresis H/E_L (%)	Nominal Registration Ratio $M(\text{soil}) + M(\text{hydrostatic})$	Nominal Overregistration (%)	Secant Registration Ratio	Secant Overregistration (%)
I (4 arms)	14	Hydrostatic	1	3	0-500	0.0137	0.0142	0.0142	3.6	3.6	0	-	-	-	-
I (3 arms)	15	Hydrostatic	2	3	0-500	0.0256	0.0266	0.0266	3.0	3.0	0	-	-	-	-
I	-	Soil	1	7	0-400	0.0242	0.0256	0.0282	9.1	22.0	13.0	0.95	-5	0.96	-4
IA	16	Hydrostatic	1	2	0-500	0.0152	-	0.0150	0	4.0	4.0	-	-	-	-
IA	-	Soil	1	3	0-400	0.0144	-	0.0153	0	6.7	6.7	0.55	-5	-	-
IA	-	Soil	2	6	0-500	0.0177	-	-	1.9	5.6	5.6	1.15	+15	-	-
IA	-	Soil	3	3	0-500	0.0175	-	0.0182	2.1	4.2	2.1	1.14	+14	-	-
IB	28	Hydrostatic	1	3	0-500	0.0378	-	-	0	0	0	-	-	-	-
IB	-	Soil	2	4	0-500	0.0375	0.0386	0.0413	2.0	6.6	4.6	0.99	-1	1.02	+2
IB	29	Soil	3	5	0-500	0.0383	0.0390	0.0420	3.8	11.5	9.6	1.015	+1.5	1.03	+3
IB	-	Soil	4	8	0-500	0.0316	0.0327	0.0345	4.2	9.0	4.8	0.84	-16	0.87	-13
III	-	Hydrostatic	1	3	0-500	0.0159	-	-	1.3	Large	Large	-	-	-	-
III	19	Soil	1	5	0-400	0.0129	-	0.0141	2.0	2.2	20.0	0.81	-19	-	-
UNM	23	Hydrostatic	1	3	0-450	0.0250	-	-	0	0	0	-	-	-	-
UNM	24	Soil	1	4	0-400	0.0334	-	-	2.6	3.8	3.8	1.34	+34	-	-
UNM	-	Soil	2	2	0-500	0.0245	-	-	1.6	7.0	7.0	0.98	-2	-	-
UNM	-	Soil	3	4	0-500	0.0365	-	0.0230	5.0	4.0	7.0	1.46	+46	-	-

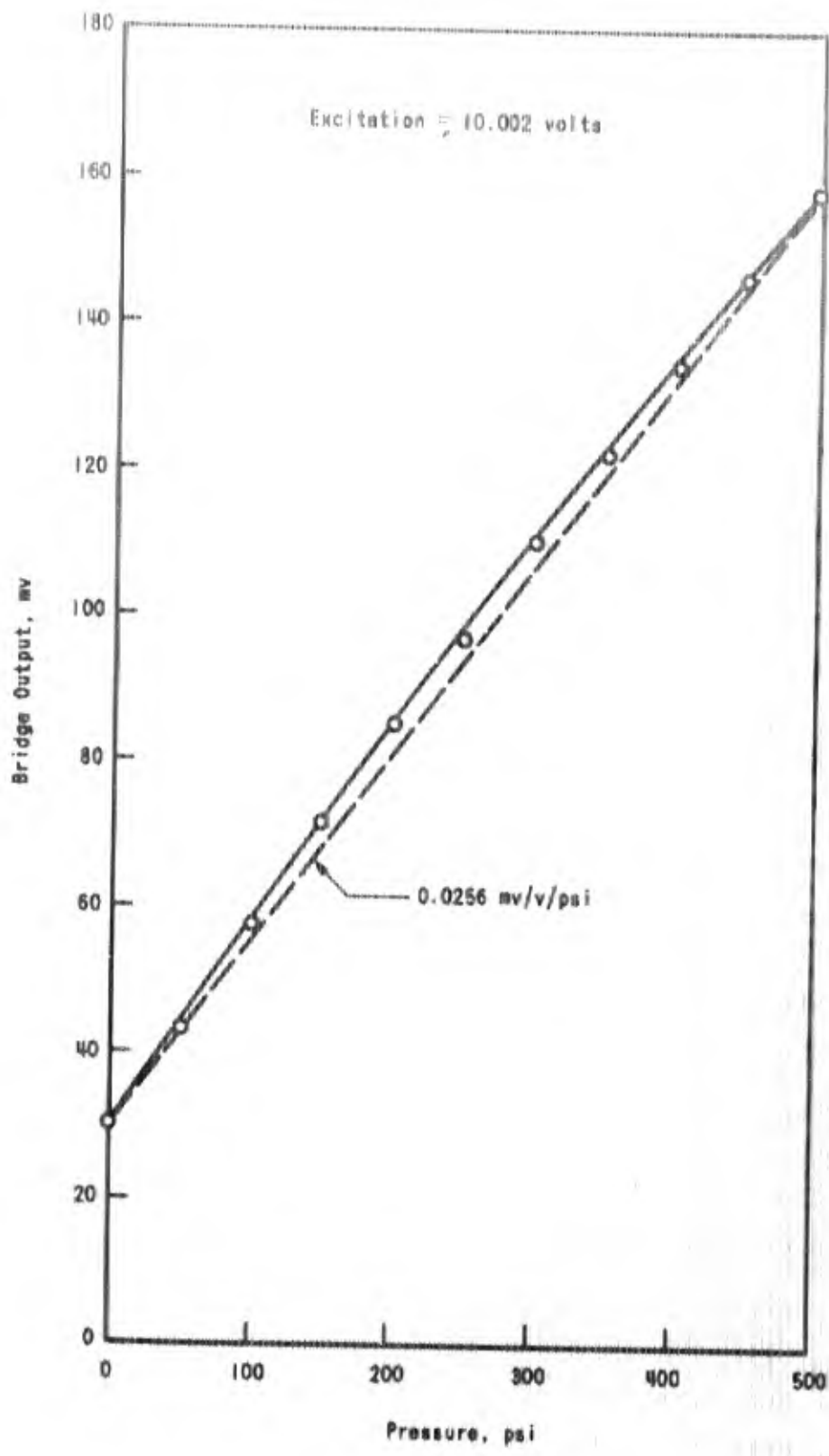


Figure 14. Hydrostatic Calibration of Model I Diaphragm Gage with Three Active Arms

The gage with three active arms was then embedded in sand in the pressure vessel at a depth of approximately 3-1/2 in. A characteristic response curve for one load cycle in the range from 0 to 400 psi is shown in Figure 15. The nonlinearity and hysteresis were significant, about 10 percent for the former in the load portion and 13 percent for the latter (Table VI). This suggests that the diaphragm might not be stiff enough. The registration ratio for this gage (calibration in soil divided by calibration under hydrostatic pressure) ranged from 0.95 to 0.97, hence the gage indicated very closely the applied stress in the soil.

Most of the difficulties appeared to be associated with the semiconductor strain gage used with Model I. An additional deflecting diaphragm gage, Model IA, was therefore fabricated. The original gage design with a 0.75 in. diameter diaphragm was used (Figure 16). This gage utilized dual element epitaxial sensors* whose resistance was 1000 ohms and whose gage factor was 100. Two such elements were connected across the center of the diaphragm while two were aligned along a radial line near the edge of the diaphragm. Based upon the theoretical considerations given in Section IV 3, it was found that the compressive strain to which the edge-located sensors were subjected should be approximately equal to the tensile strain to which the gages at the center of the gage would be subjected.

The physical characteristics of this gage are given in Table V, page 52. The thickness-diameter ratio was 0.112, the area ratio was 0.14, the density was 460 pcf and the diaphragm diameter-deflection ratio was 5600.

The hydrostatic calibration curve for gage IA is shown in Figure 17. The response is linear during loading, but shows some hysteresis and nonlinearity upon unloading, about 3.7 percent (Table VI, page 54). The reason for this hysteresis has not been

* GE Type 4SN306 R1000.

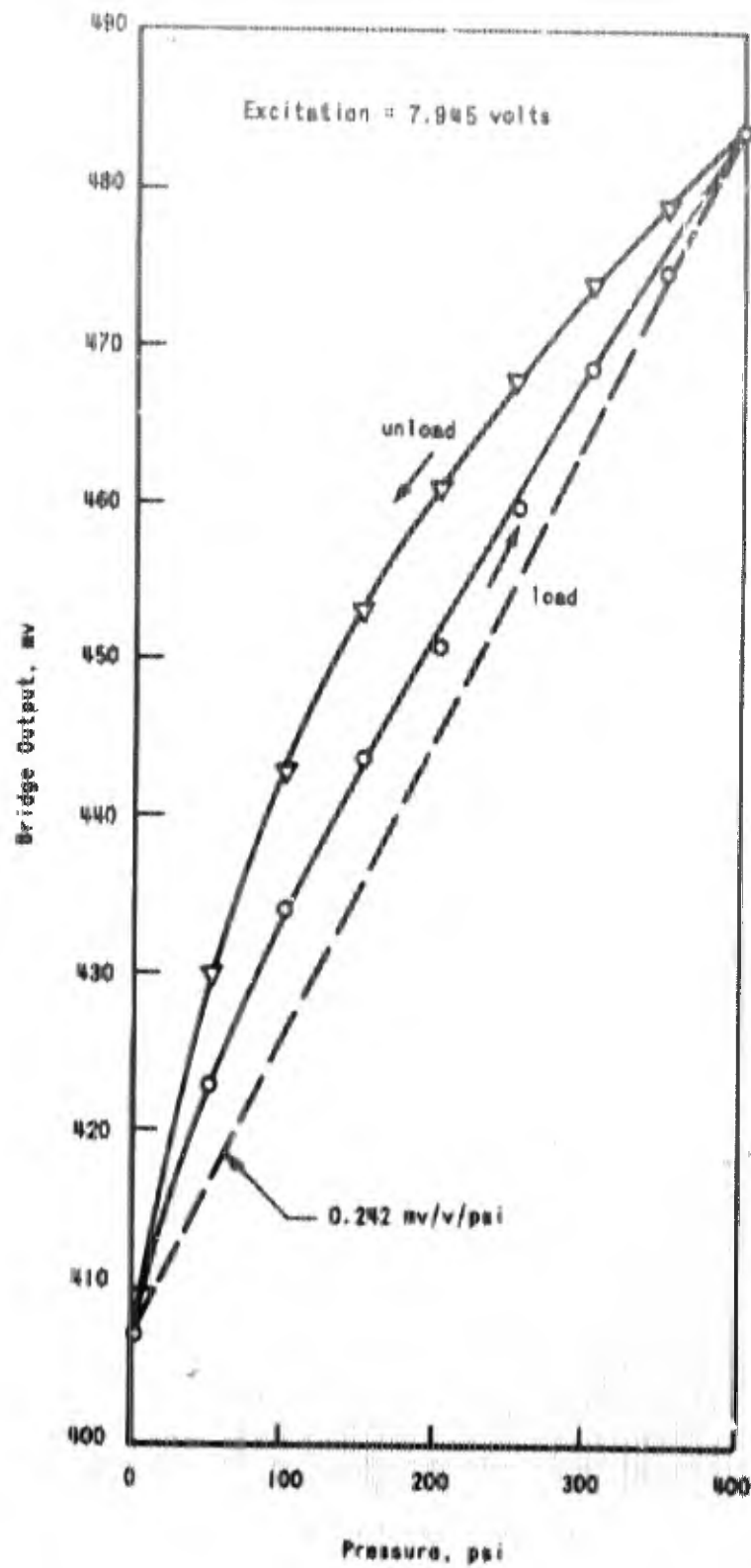


Figure 15. Soil Calibration of Model I Diaphragm Gage with Three Active Arms

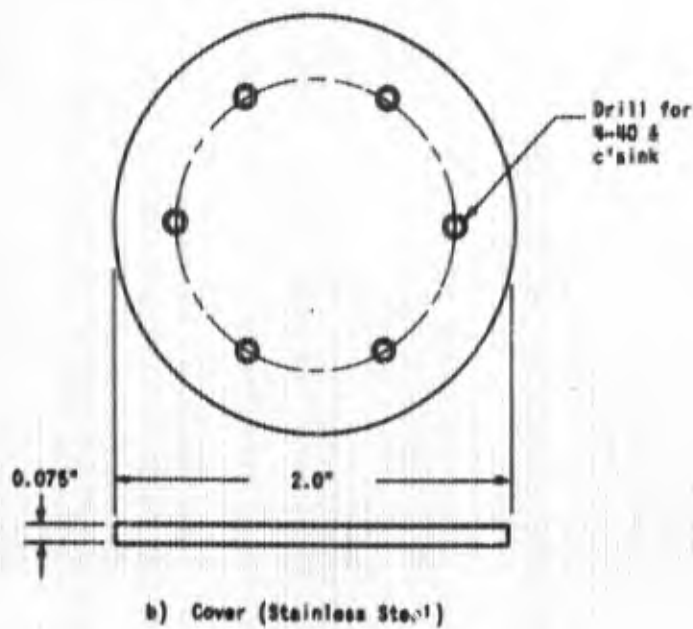
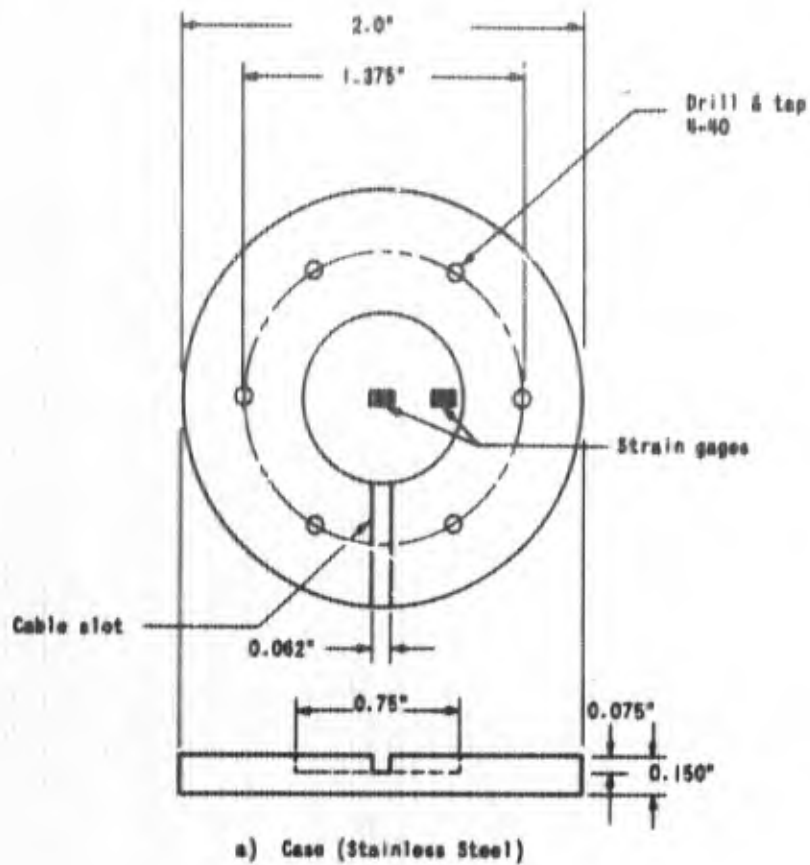


Figure 16. Diaphragm Gage - Model IA

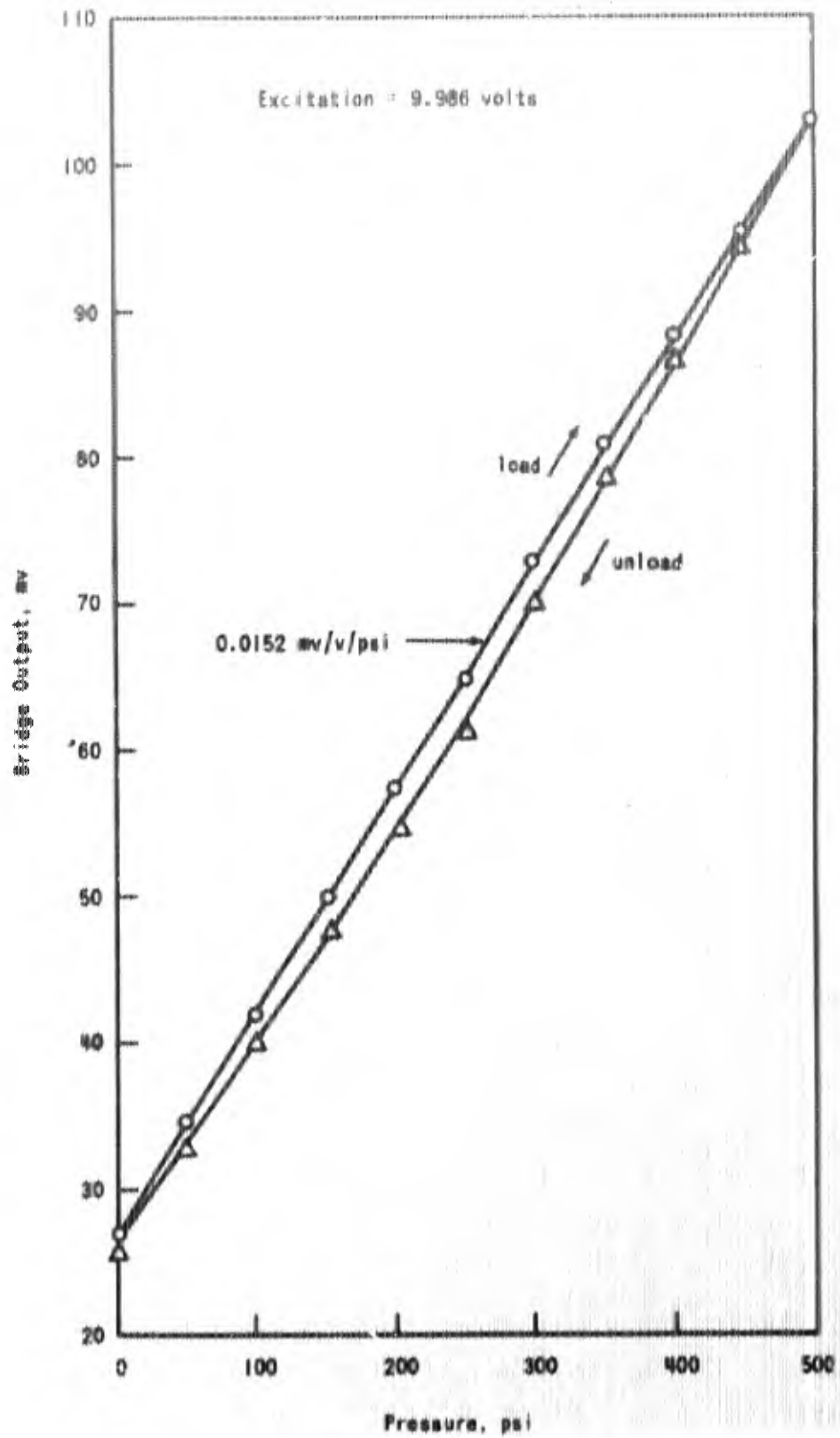


Figure 17. Hydrostatic Calibration of Model IA Diaphragm Gage

determined. The calibration curve is reproducible. The magnitude of the bridge output was not as large as calculated. Subsequent investigation showed that the strain gages near the edge of the diaphragm were not changing as much as they should have, apparently because they were not in the precise position intended.

The results of the tests in soil for gage IA are summarized in Table VI. A typical curve is shown in Figure 18. The response upon loading was quite linear. The nonlinearity upon unloading was about 5 percent and the hysteresis slightly less. The ratio of calibration in soil to calibration under hydrostatic pressure ranged from 0.92 to 1.17, hence showing a tendency to overregister on the average of about 10 percent (Table VI). The behavior exhibited by this gage in soil suggests that diaphragm-type gages can work in soil if properly designed.

3. BEAM GAGE

The next concept considered was a simply supported beam design, which is based upon theoretical considerations given in Section IV 5. The drawing for this gage (Model III) is shown in Figure 19. The physical features of this gage are given in Table V, page 52. The overall thickness and diameter are approximately the same as those for Model IA. As indicated in Figure 19, the beam is placed in the cavity of the body and is confined so as to restrict its motion to only several thousandths of an inch in any direction, except by bending. The beam is loaded by a knife edge at the middle which is attached to the center of the cover. The stiffness of Model III is probably less than that of Model IA since the beam probably does not compensate for the reduced thickness of the diaphragm.

Initially, it was planned to fabricate the beam completely of silicon. It was decided, however, to make initial checks using commercial piezoresistive strain gages bonded to a steel beam, because of fabrication problems encountered with the solid piezoresistive elements. Two such gages were placed on the top of the beam, and two at the bottom. In operation, the upper strain gages

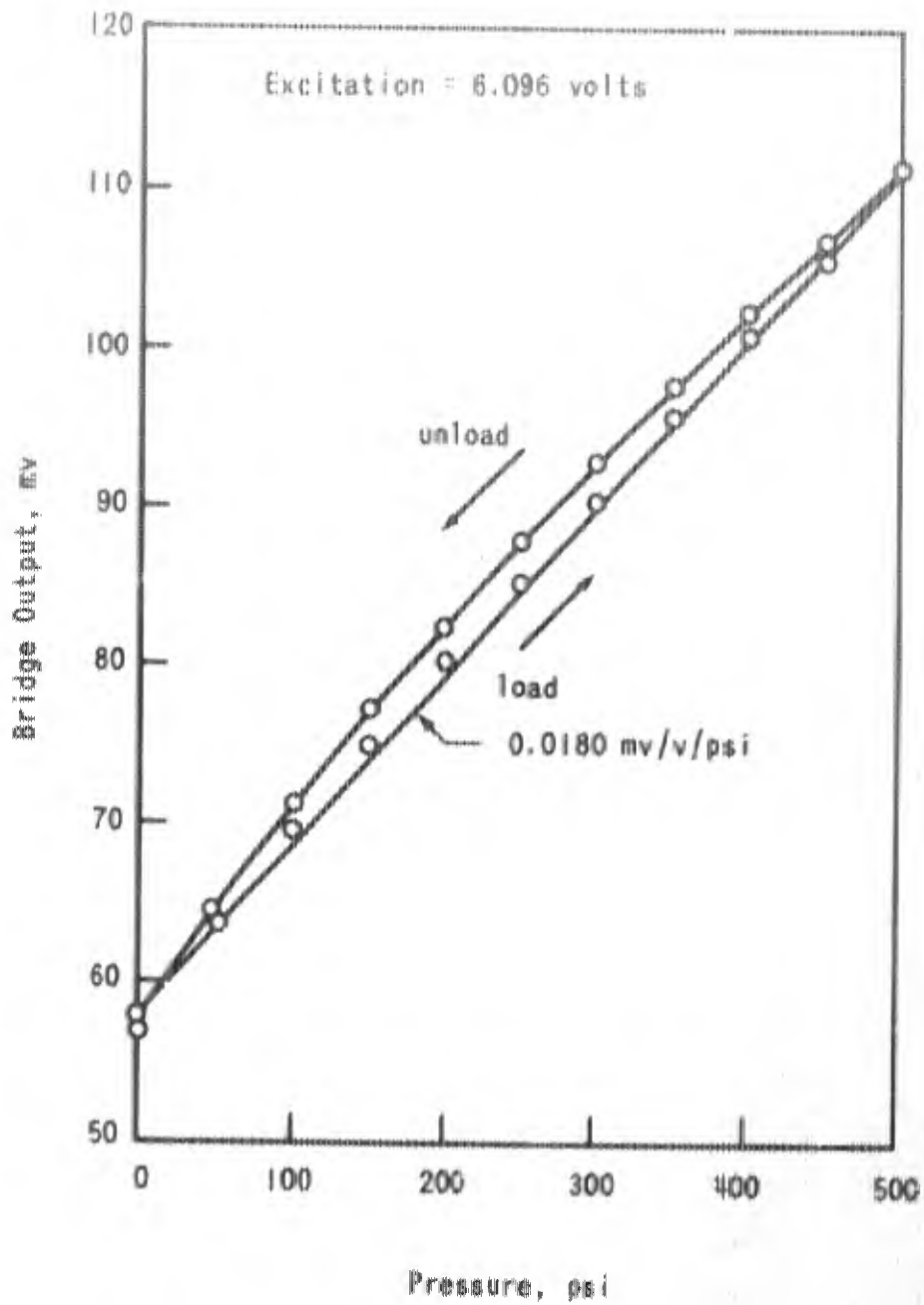


Figure 18. Soil Calibration of Model IA Diaphragm Gage

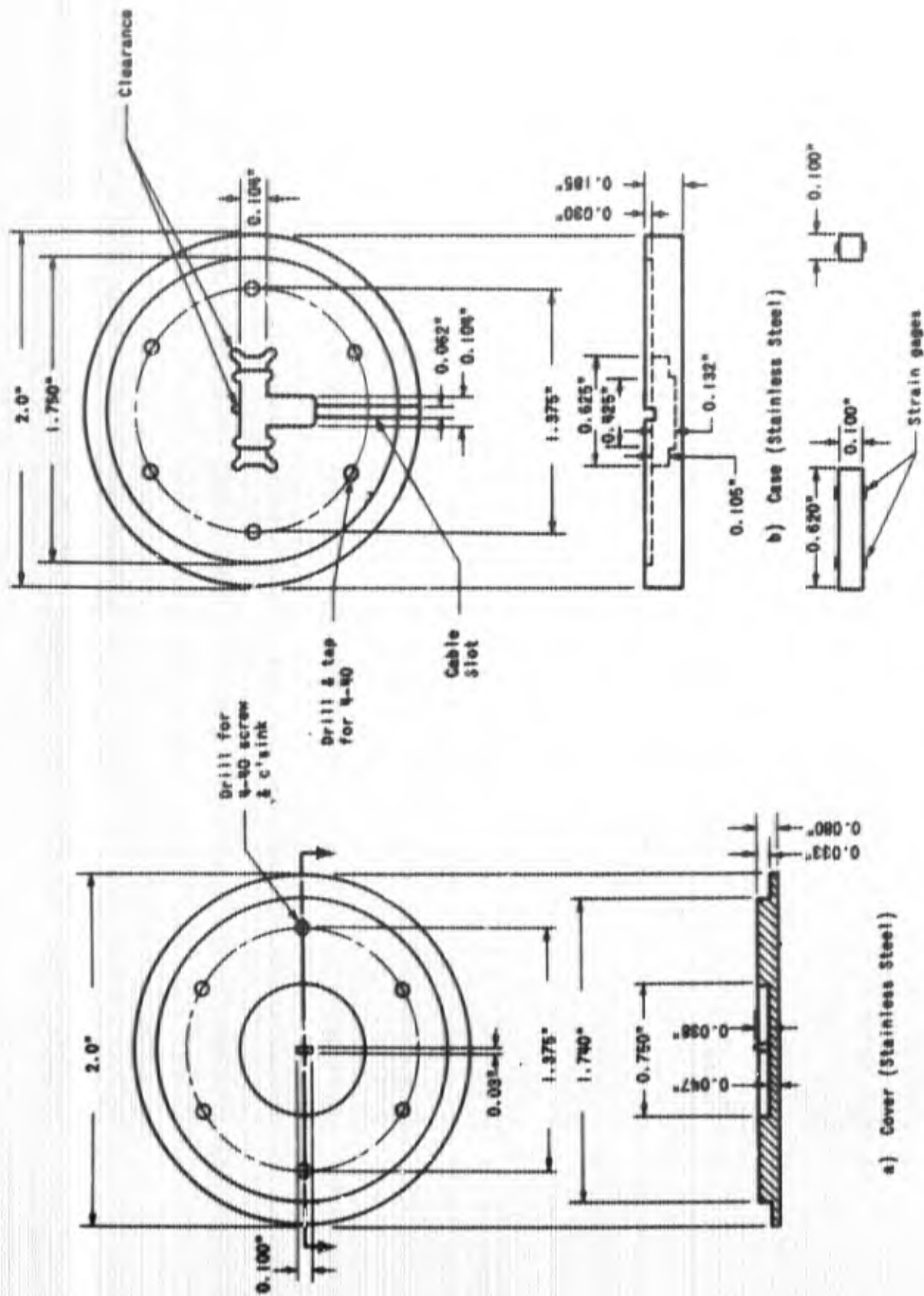


Figure 19. Beam Gage - Model III

would be subjected to compressive strain while the bottom strain gages would be subjected to a tensile strain. The connection of the four strain gages in a bridge would give an output directly proportional to the percentage change in resistance. The knife edge was ground to such a height so as to make slight contact with the beam when the cover and case were assembled.

The commercial strain gages selected to be used with the beam gage were four single-element, silicon-backed, epitaxial strain sensors.* The resistance of each element was 1000 ohms and the nominal gage factor was 100. It was decided to attempt to solder these gages in place as it was felt this might lead to a more secure bond and eliminate some problems of induced strain in the element. The beam was first tinned with tin gold solder. This was done selectively to prevent tinning the area under the knife edge, and to prevent any solder from running onto those areas of the beam that rested on the supports in the case. Solder at these locations was undesirable since smoothness would be needed to ensure linearity in the performance of the gage.

The solder used in assembly was a eutectic mixture of gold and tin. This solder was recommended by the manufacturer of the strain sensors for strain levels between 500 and 1000 microstrain. Each of the four sensors was fastened the same distance from the center of the beam. Thus, the strain to which each element was subjected should be equal. However, one strain gage became damaged in assembly so the fabricated gage used for evaluation of the concept had only three active arms. An external balancing resistor was used in the bridge in place of the missing active arm.

The results of the hydrostatic calibration are given in Figure 20. On the first cycle the response was reasonably linear up to about 350 psi. As the pressure increased above 350 psi, the rate of change in voltage output decreased rapidly. Unload response was reasonably linear down to 150 psi. There was

* GE Type 4SN303 R1000.

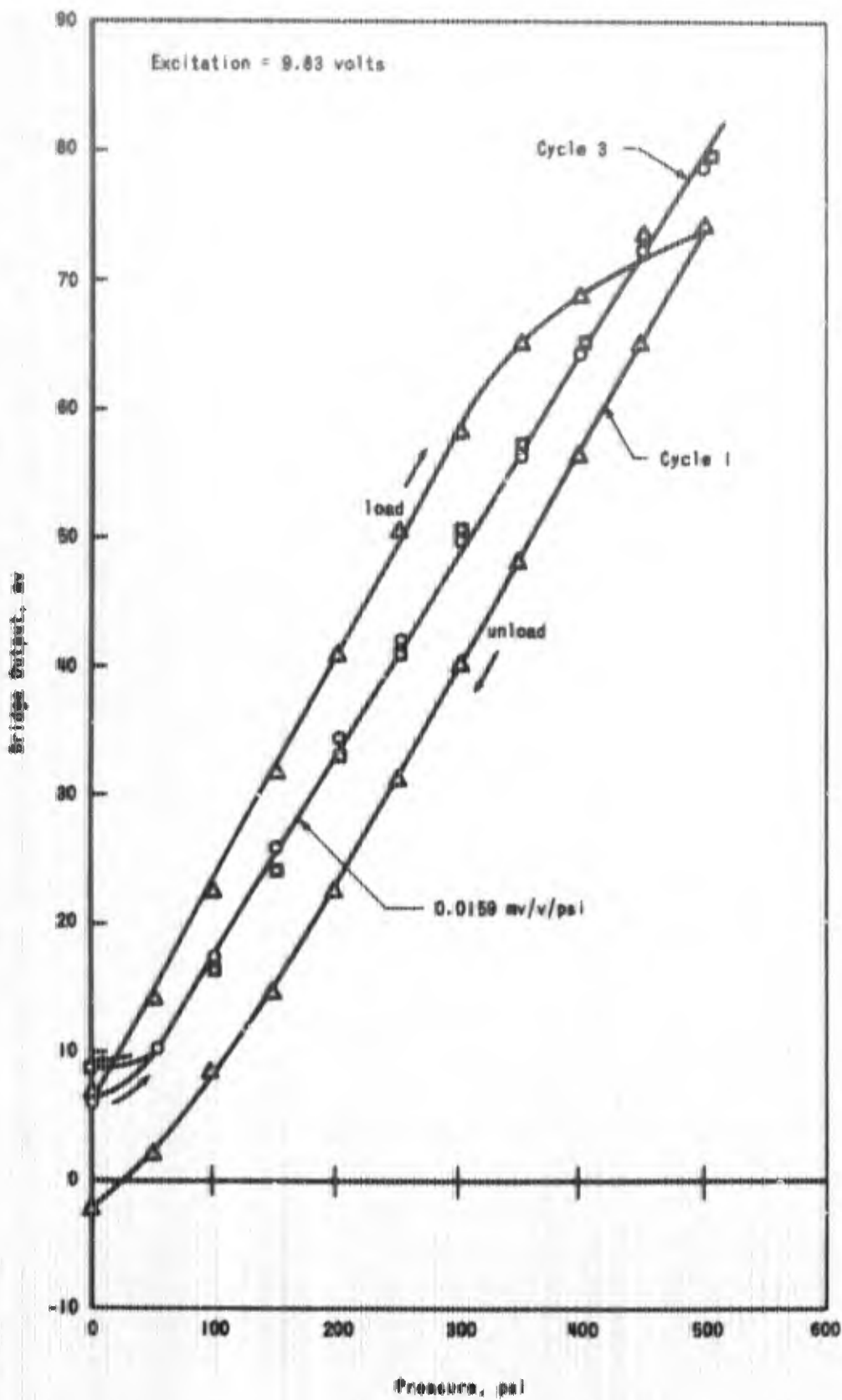


Figure 20. Hydrostatic Calibration of Model III Beam Gage

considerable hysteresis in the first cycle. Subsequent inspection of the gage showed that this response was caused by indentation of the beam by the knife edge caused by high stress concentrations under load.

On the third load cycle, about 50 psi was required before significant response occurred, indicating that this much pressure was required for the knife edge to make contact with the indentation. At higher pressures the response was linear with little hysteresis.

The behavior of this gage in soil is shown in Figure 21. There was no output change from 0 to 50 psi, however, response was linear during increase in stress above 50 psi. Unloading was approximately linear, but with a different sensitivity. The registration ratio was 0.81 indicating a 19 percent underregistration.

4. COMPRESSION GAGE

A gage (Model II) using the transverse piezoresistive coefficients described in Section IV 4 for an element in direct compression, was designed and fabricated. Figure 22 shows the dimensions of the gage case. The physical characteristics are given in Table V, page 52. The overall thickness-diameter ratio was 0.112, the sensing area ratio was 0.14, the density was about 485 pcf and the stiffness much higher than that of the other models.

Since no commercial transducers using the transverse piezoresistive effect were available, it was necessary that they be constructed at IITRI. Single crystal silicon rod was ordered for this purpose. This rod is oriented with the [111] direction along the rod axis. The gage design shown in Figure 22 allows for rectangular slices of silicon to be placed between the top plate and the raised circular post in the center of the gage body. The dimensions of the post allowed for a sensor width of approximately 0.04 in. and a length of approximately 0.16 in. For a 0.006 in. thick slice of this silicon with the cross-sectional area indicated, the resistance of the sensing element would be approximately 3000 ohms.

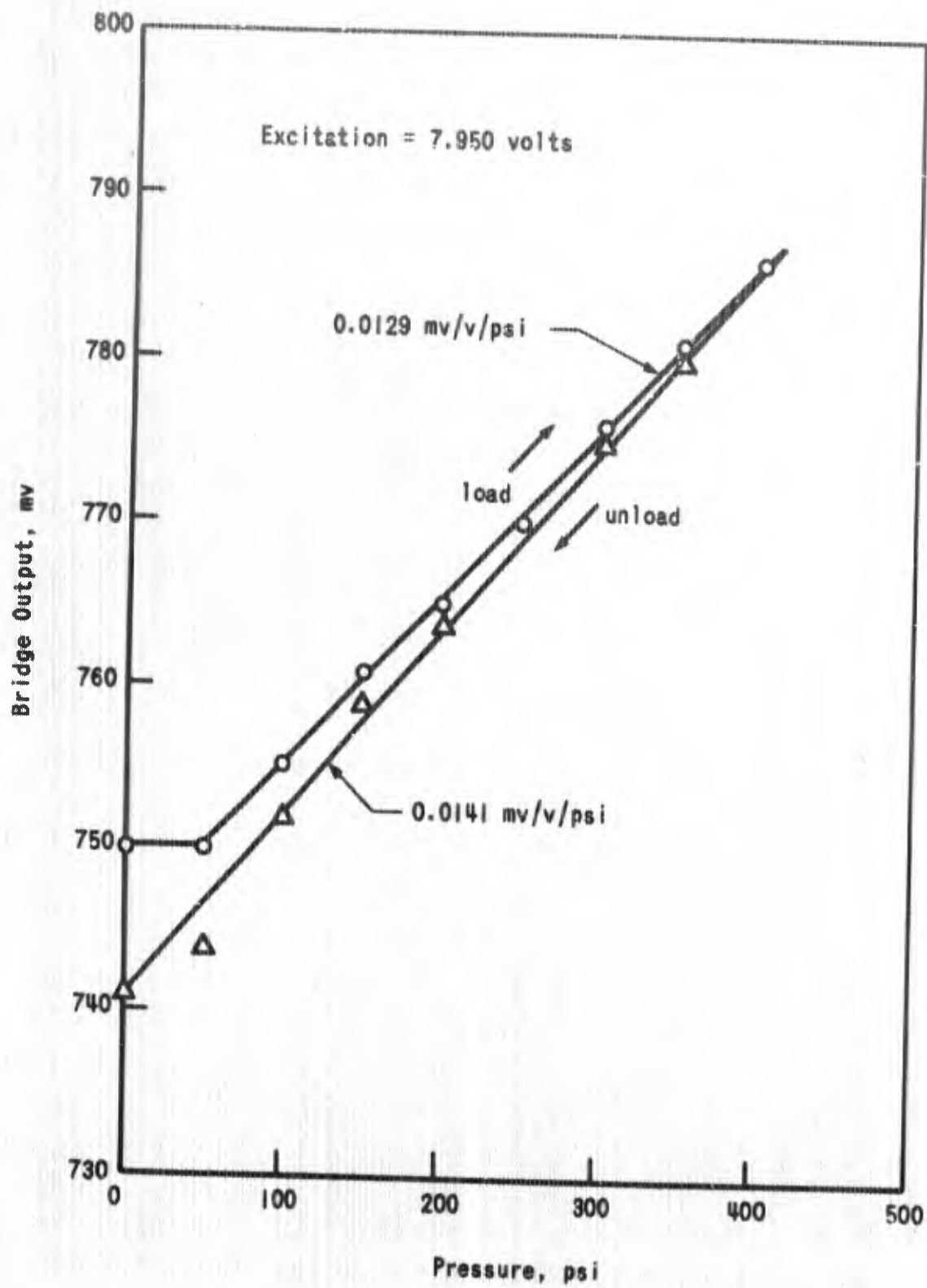


Figure 21. Soil Calibration of Model III Beam Gage

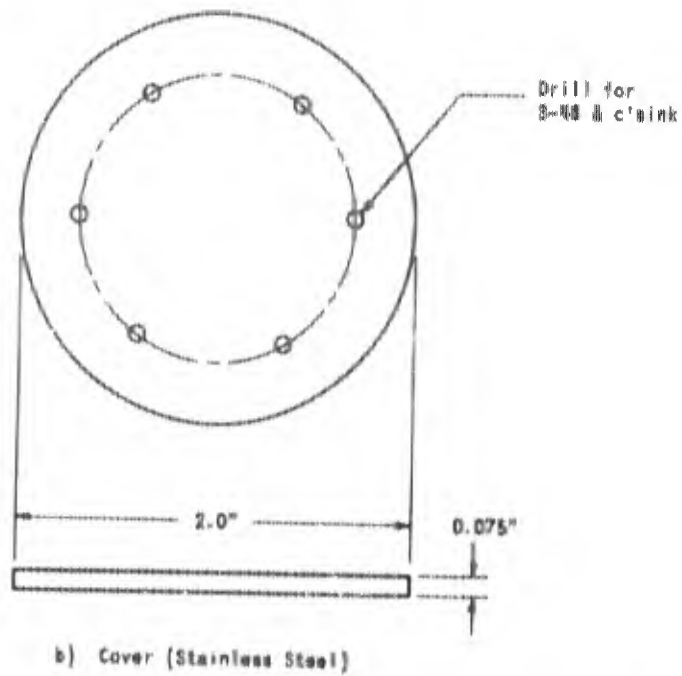
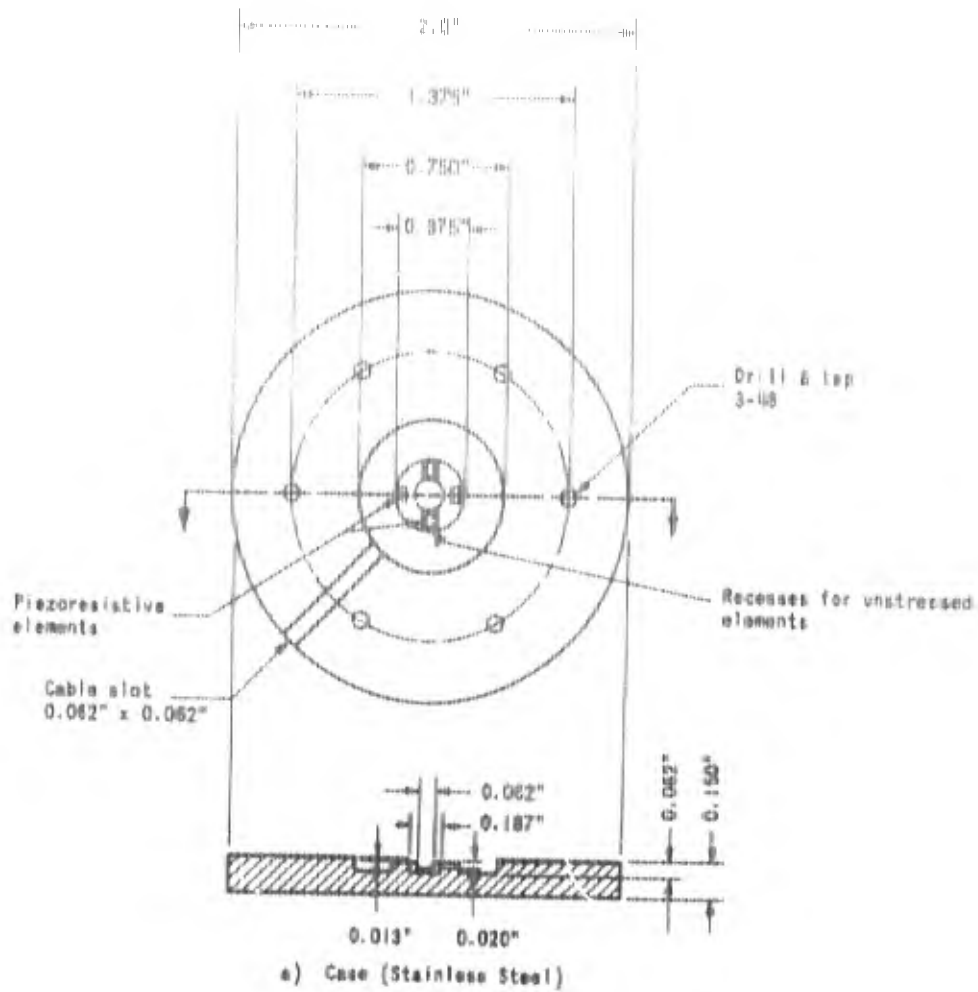


Figure 22. Compression Gage - Model II

In order that a properly oriented silicon sensor be cut from the rod, it was necessary to precisely locate the crystal axes in the silicon rod. The equations show that optimum sensitivity is obtained if the sides of the rectangular parallelepipeds used are parallel to the faces of the silicon crystal. The procedure used to obtain the sensing elements was as follows: X-ray crystallographic measurements were made of the rod in order to locate the crystal axes. The rod was mounted in an X-ray fixture that is capable of being adjusted in three orthogonal directions. X-ray photographs were taken and the orientation of the rod adjusted until the (100) face of the crystal was in a vertical direction. The [100] axis was then parallel to the base of the fixture. A diamond saw was used to slice the rod in the vertical direction. For alignment purposes, a horizontal slice was made in the exposed face. An additional vertical slice removed a small portion of the rod. A thicker slice was made in the rod and a specimen obtained that had a thickness, after lapping, of 0.042 in. with an axis orientation line on the surface.

The section of the rod thus obtained was affixed to a glass slide mounted on a lapping block. Cuts parallel to the orientation line were then made 0.160 in. apart. The resulting rectangular slices were mounted between two pieces of slide glass on a second steel block. Additional slicing was performed to obtain the required rectangular parallelepiped. The resulting pieces were lapped to their final size of 0.016 in. by 0.042 in. by 0.013 in.

The original gage design called for slices that were 0.006 in. thick. It was found to be very difficult to lap to this small thickness; therefore, the thickness of the slices was increased to approximately 0.013 in.

Electrodes were required on each end of each of the slices in order to allow leads to be attached. It was found rather difficult to place these electrodes. Initial attempts were made to

deposit gold films on the ends of the specimens. Conventional cleaning techniques were apparently unsuccessful in removing all of the grease from the surface of the silicon. The result was that the gold films were found to peel away from the silicon when removed from the vacuum chamber. Successful contact was finally achieved by wetting the ends of the pieces of silicon with indium by means of an ultrasonic soldering gun. Gold wire connections were then made to the indium.

The gage case itself was machined to have a surface smoothness of 0.5 microns. A one micron film of sodium monoxide was applied to those surfaces of the gage case that would be in contact with the silicon chips, so as to provide insulation between the silicon and the metallic case. Epoxy was then placed on the gage body and the silicon chips appropriately located. Two of the chips were placed on the circular posts and subjected to loading from the diaphragm. An additional two were placed in recesses so as not to be subjected to any strain when the gage was placed under pressure. These two unstrained elements were to act as temperature compensating arms and not change in resistance at all as a result of the applied strain. The four elements were connected in a four-arm bridge.

Considerable effort was devoted to the development of techniques for fabricating a suitable gage using this direct compression concept. The results were not successful. Response in soil and under hydrostatic pressure was erratic. An example is given in Figure 23. Much of the difficulty probably lies in the development of stress concentrations at the contact surfaces between the piezoresistive elements and gage case. In addition, the properties of the piezoresistive elements were changed by the method of connecting the leads. This may have caused the hysteresis.

A load test of a single piezoresistive element in direct compression was made to evaluate its response characteristics. The element was identical to those used for the arms of the

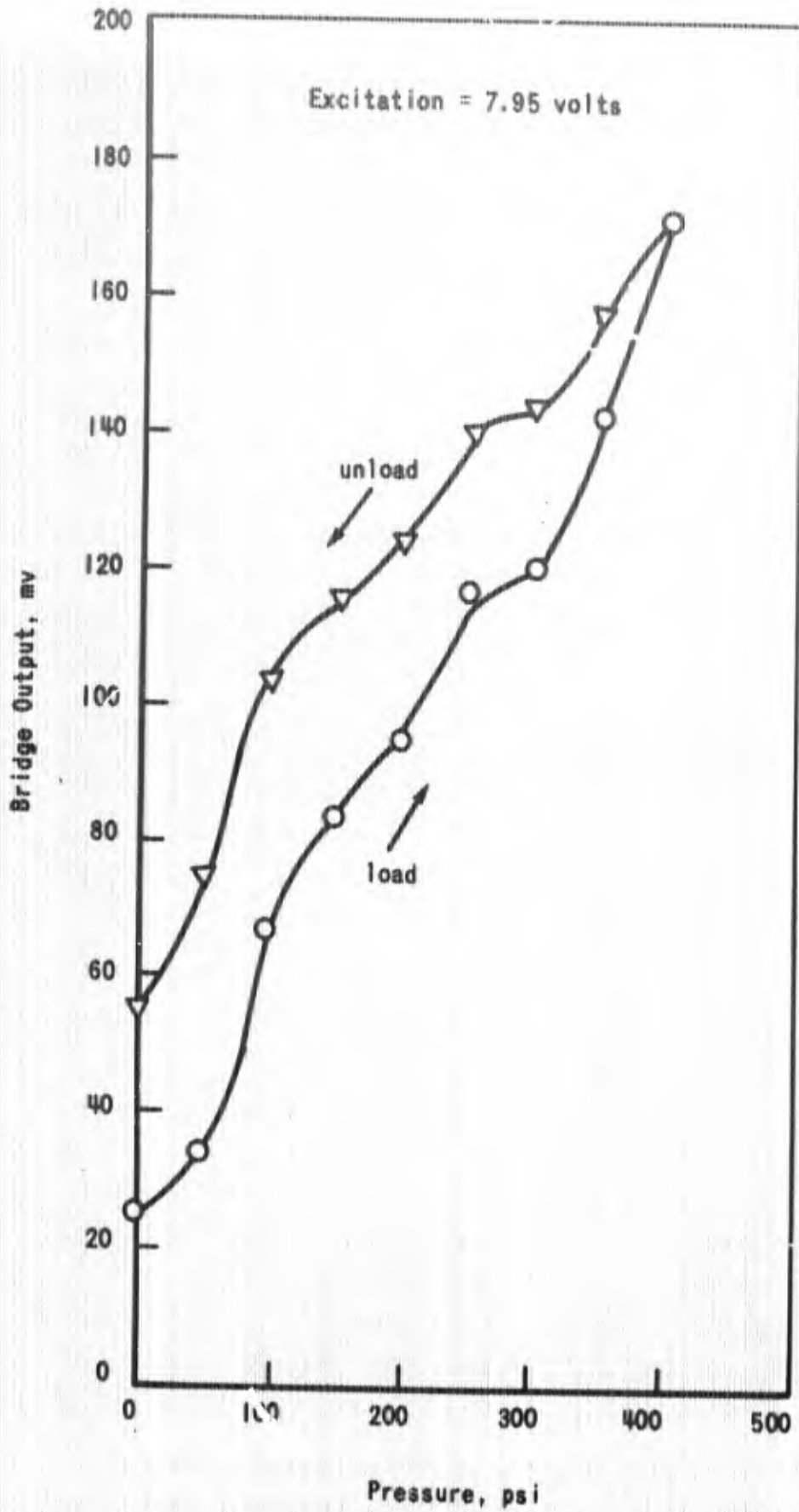


Figure 23. Soil Calibration of Model II Compression Gage

direct compression gage. The element was placed in a testing machine between two platens and cushioned by teflon sheets. The element fractured at a 132-lb load. Based on the size of the element, this load represents an average stress in excess of 20,000 psi. The results in Figure 24 show that the direct compression concept can work.

5. UNM GAGE

The physical characteristics of the UNM gage are given in Table V, page 52. The thickness-diameter ratio was 1.33, the sensing area ratio was 0.31, the density was about 91 pcf, and the stiffness very high.

Its response under hydrostatic pressure was linear and reproducible with no hysteresis (Figure 25). The gage was also tested in soil with the sensing element placed upward about 3 in. from the soil surface. Although the nonlinearity and hysteresis were not generally large (Figure 26), the calibration constants varied over a wide range (Table VI, page 54). For three separate placements the registration ratios varied from 0.98 to 1.54, much larger than for any of the other gages tested. It appears that the gage, in general, overregisters by a significant amount and is sensitive to placement. This is consistent with the theories on effect of adverse gage thickness-diameter ratio, i.e., greater than 1. The small nonlinearity and hysteresis is probably attributed to the very high stiffness of the gage.

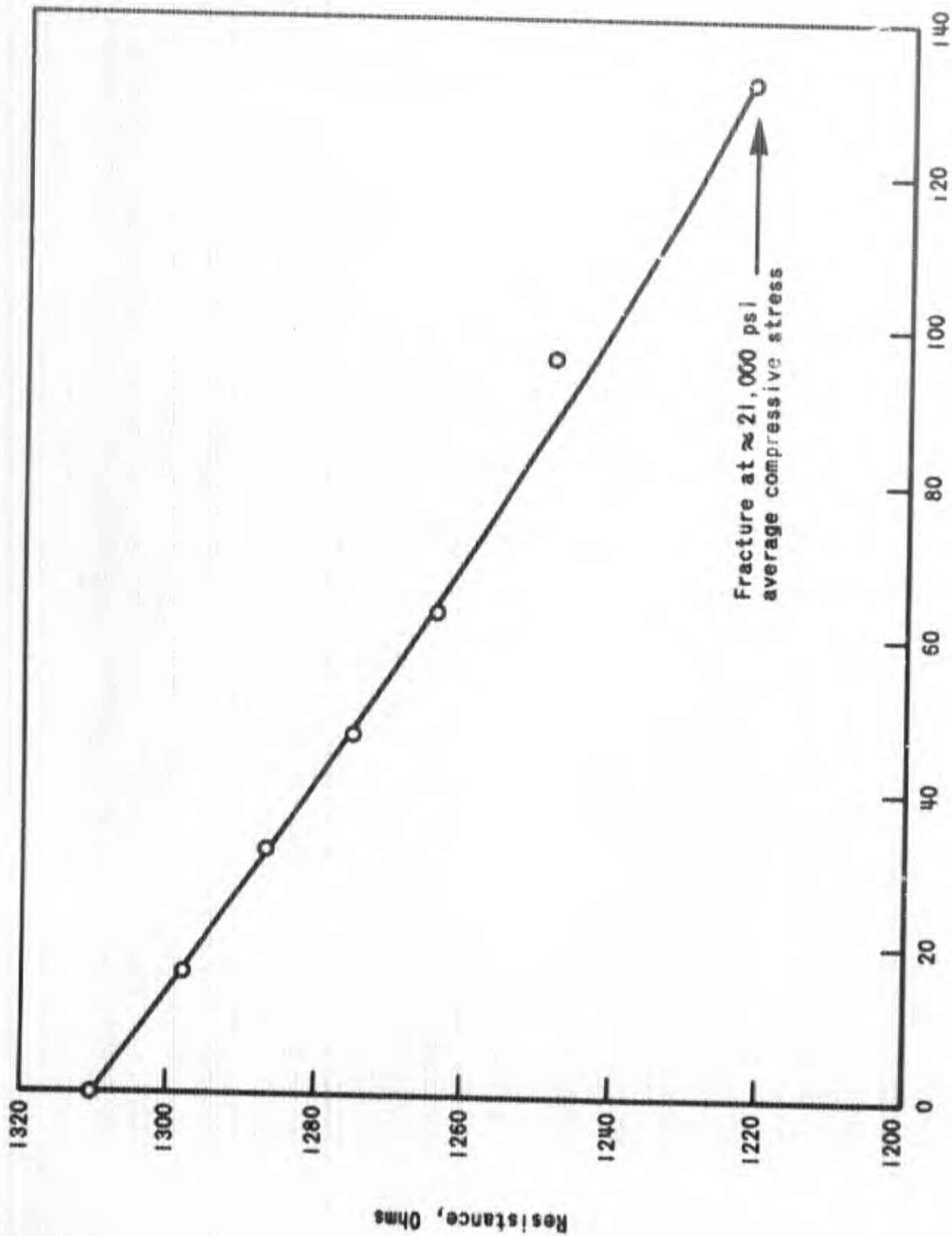


Figure 24. Response of Silicon Element in Direct Compression

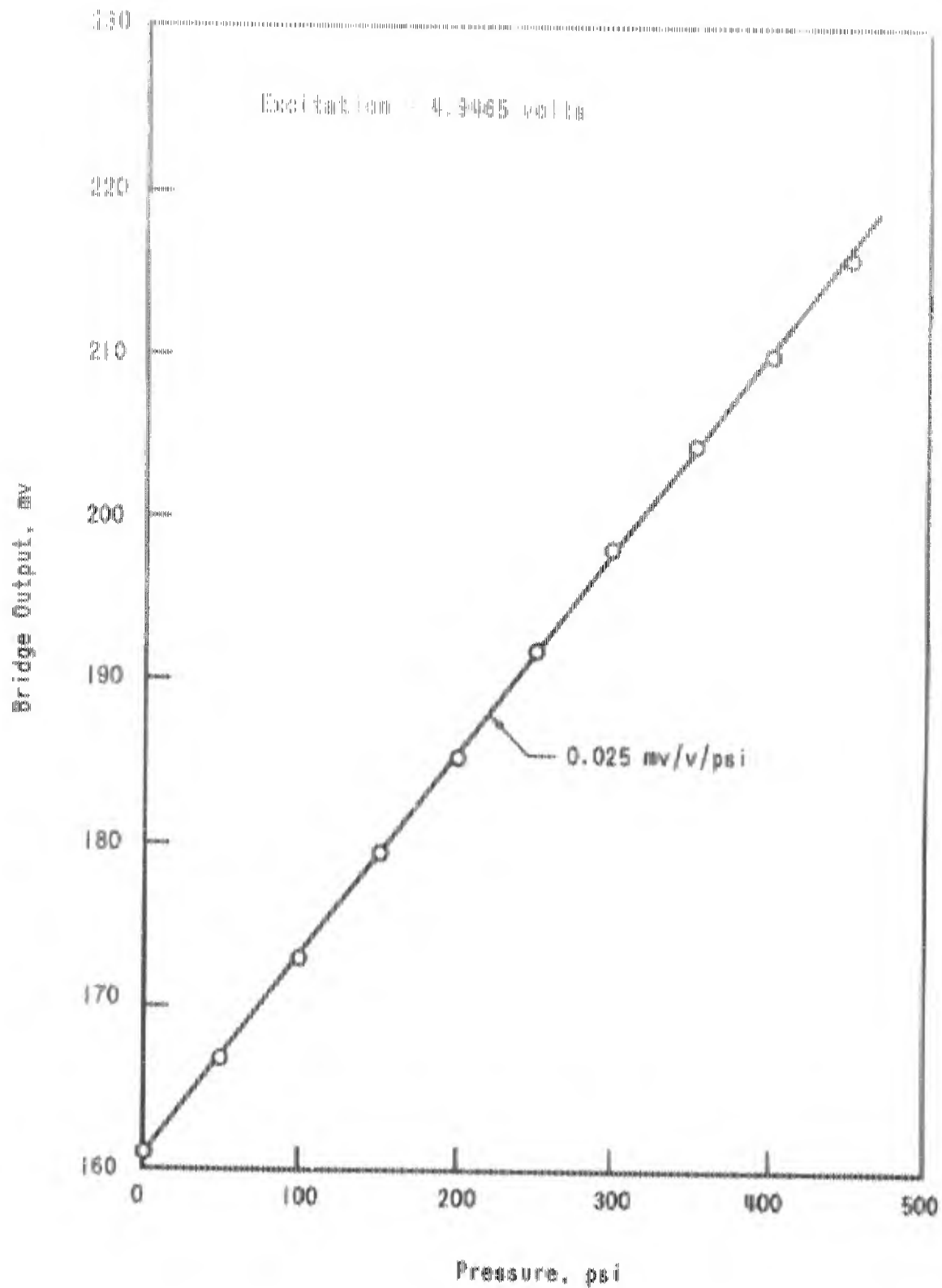


Figure 25. Hydrostatic Calibration of UNM Soil Stress Gage

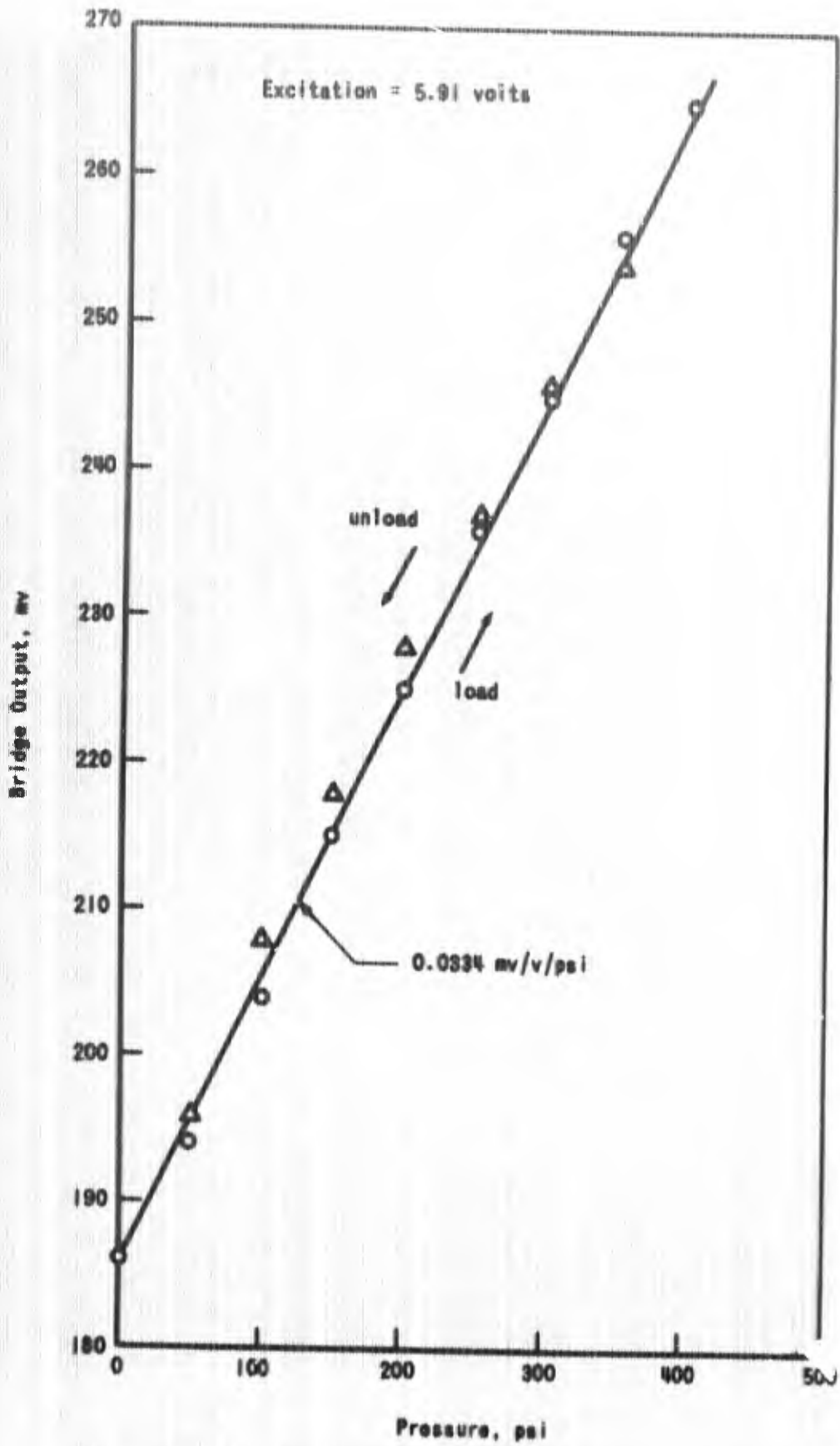


Figure 26. Soil Calibration of UNM Soil Stress Gage

SECTION VI
FINAL DESIGN

1. CONSIDERATIONS

The results of the preliminary gage investigations discussed in Section V are summarized by Figure 27 and in Tables V and VI, pages 52 and 54. On the basis of these results, the deflecting diaphragm concept appears to be the most promising of those investigated. As Model IA showed, this concept can provide a reasonably linear response in soil with satisfactory sensitivity and a reasonable indication of the correct stress. Model I, although the same as Model IA except for diaphragm diameter, was considerably inferior to the latter in linearity and hysteresis. This may be attributed directly to the difference in diaphragm stiffness between the two. Neither gage is close in density to that of soil so further modification would be required for satisfactory dynamic response.

The beam gage, Model III, developed considerable hysteresis probably as a result of local yielding at the contact points between the beam element and the knife edge or supports. This could be eliminated, for the stress range under consideration, by a larger contact area. However, the gage was elaborate and hence difficult to machine. The frequency response characteristics under dynamic load is also difficult to predict. All factors considered, there appears to be no offsetting advantage in this concept over the much simpler deflecting diaphragm concept. Consideration of a gage using a beam composed of a solid piezoresistive material does not appear worthwhile at the present.

The UNM gage does not provide the most satisfactory results. Although linearity and hysteresis are similar to those of the diaphragm gage model IA, the magnitude of response of the UNM gage varies widely in soil. The strong tendency to overregister and the apparent high sensitivity to placement may be attributed to the large thickness-diameter ratio. The fact that the gage is

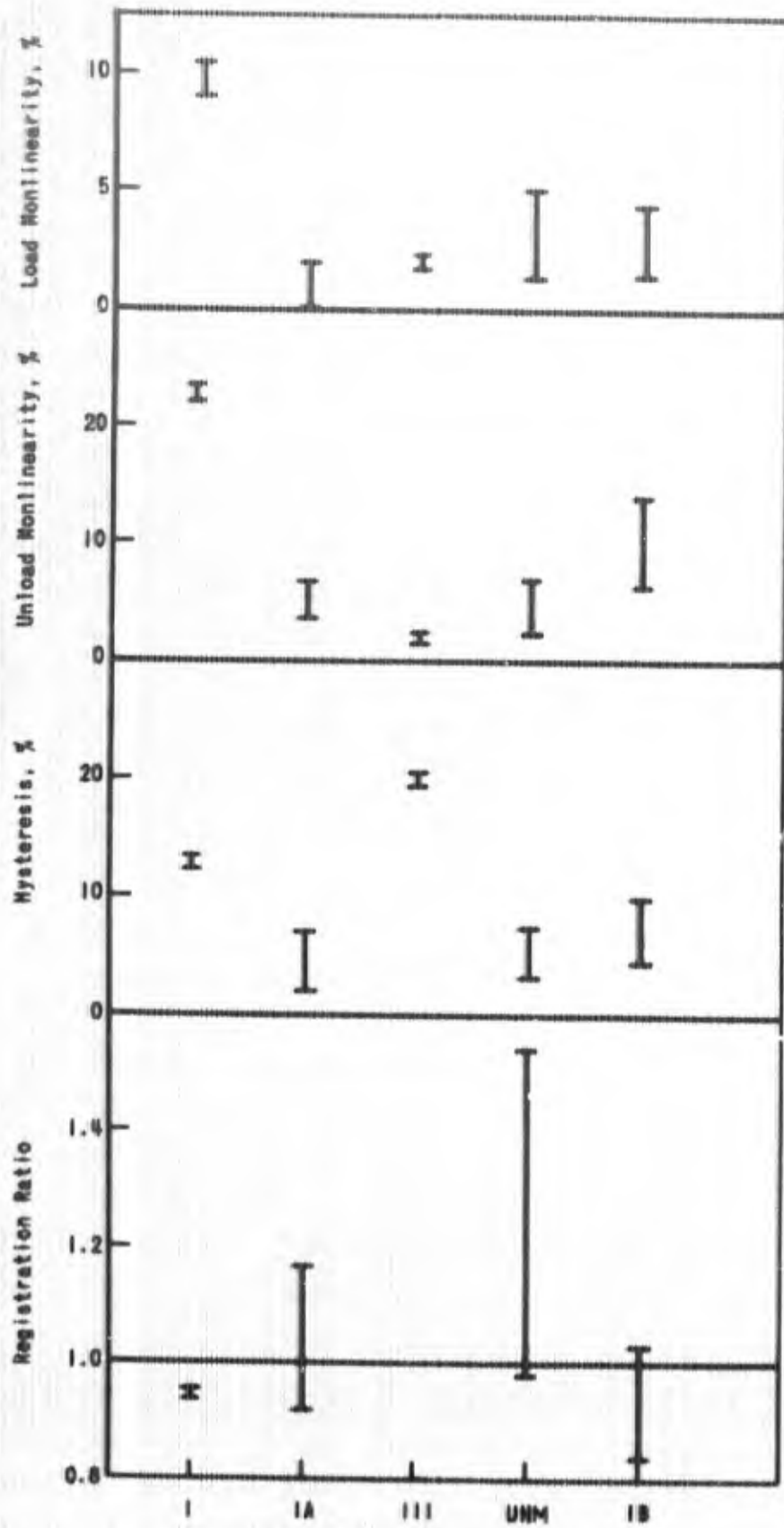


Figure 27. Summary of Gage Response in Soil

at the same time very stiff was probably responsible for maintaining the linearity and hysteresis within a reasonable range.

Theoretically the direct compression element gage is a sound concept. It will provide a very stiff gage with sufficient sensitivity. However, there remain a number of fabrication problems to be resolved. Although the greatest percentage of the development effort in this study was devoted to this concept, no successful gages were achieved. Therefore, this concept could not be considered as a candidate for the hardware delivery requirement on the present study. If the feasibility of this approach is to be fully evaluated, considerably more research will be necessary.

2. DESCRIPTION OF GAGE

For the final gage design, modification of Model IA was selected as the most satisfactory approach of those investigated. Although performance characteristics of IA were acceptable under static load, a number of modifications were still desired. These were: 1) a closer matching of gage density to soil density; 2) a greater ratio of diaphragm area to total area; 3) increased sensitivity through improvement in strain gage arrangement; and, 4) a method of waterproofing the gage. The gage, illustrated in Figure 28, is designated Model IB.

It was originally planned to replace part of the outer portion of the steel case by a plastic ring to provide density matching without reducing the overall thickness-diameter ratio. This was the method used in the WES gage design. However, instead the material for gage fabrication was changed from steel to aluminum since this was a simpler method. Because of the lower Young's modulus of aluminum the diaphragm thickness had to be increased to maintain adequate stiffness. In addition, the overall gage diameter was reduced from 2 in. to 1.5 in. to improve the area ratio. It was not possible to reduce the overall thickness in proportion, so a thickness-diameter ratio increase resulted.

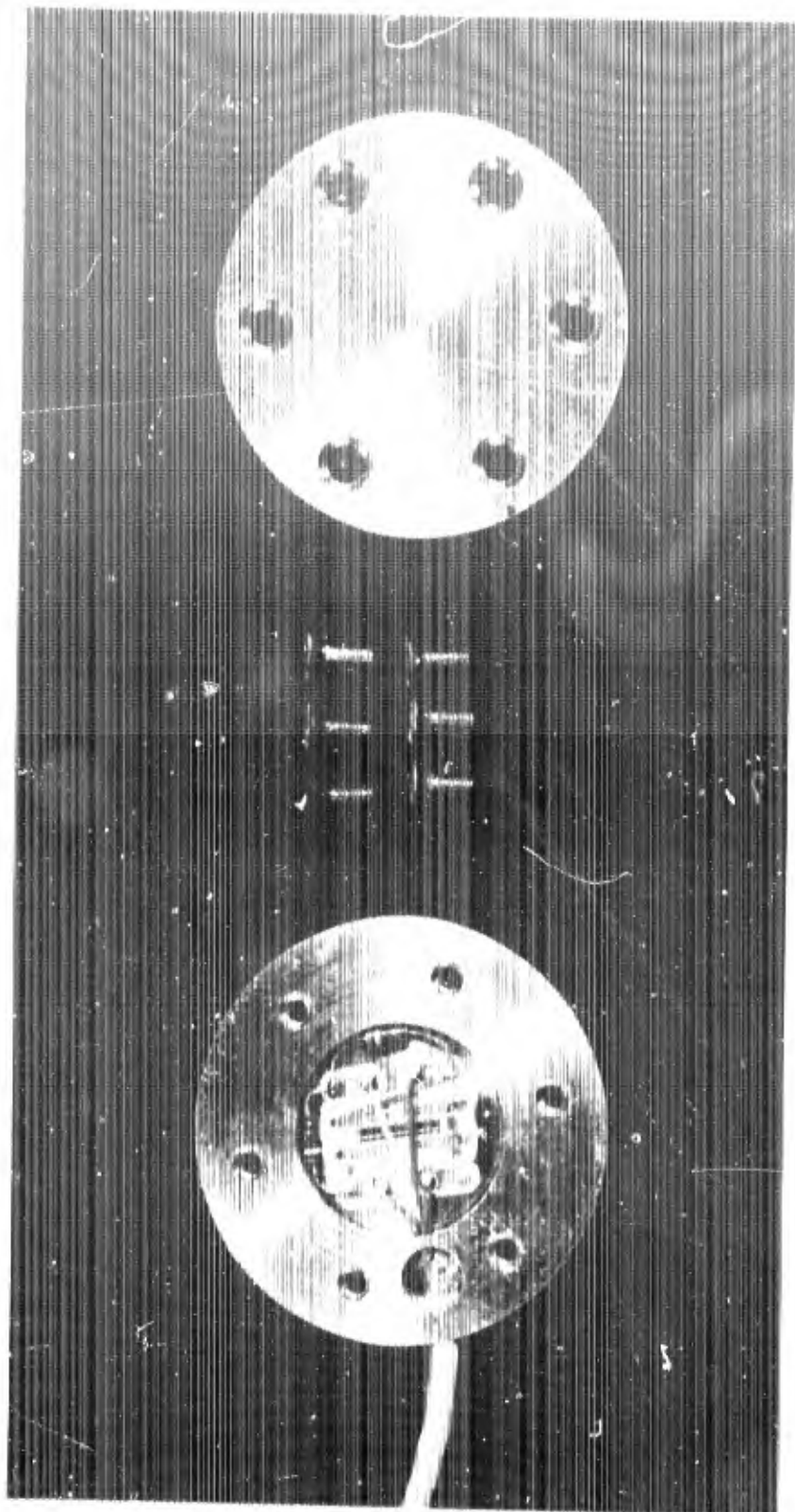


Figure 28. Diaphragm Gage Model 1B

In addition to the aforementioned features, special consideration was given to waterproofing the gage. The major problem in this regard was the cable penetration point since the cover itself is easily sealed. A well was provided in the ring around the cavity intersecting the hole for the cable. The entire cable was inserted through the radial hole connecting the outside of the gage with the well. The cable cover and shielding were stripped away at this position and only the inner insulated leads were allowed to pass into the diaphragm cavity. The well was filled with a hardening conductive epoxy serving three functions: 1) grounding the cable shielding to the gage case; 2) providing a moisture barrier between the inner leads and the outside of the gage even if the cable cover is not waterproof; and, 3) anchoring the cable to the case. The cover and body of the gage were sealed with nonhardening resin.*

A change was also made in the piezoresistive strain gages used in an attempt to eliminate the problems encountered with gages I and IA. The gages selected consisted of a two active arm p- and n-silicon combination.** The resistance of the elements was nominally 350 ohm. One such gage was mounted in the center of the diaphragm in the gage body. Only one active diaphragm was used. Both arms of the strain gage should be subjected to identical strain when pressure is applied to the diaphragm; however, one arm will increase in resistance and the other will decrease. A reasonable degree of temperature compensation should also be provided. Fixed resistors were added inside the case to provide a full balanced bridge with two active arms. The strain gages were mounted with a hardening epoxy*** and then together with the exposed wires were coated with resin* to waterproof them.

* Sylgard 182.

** Kulite Type MP 103-9.

*** Armstrong A2.

A photograph of the gage before assembly is shown in Figure 28. The strain gages and resistors may be seen attached to the gage body.

3. EVALUATION OF GAGE

The physical features of Model IB are summarized in Table V, page 52 and Figure 29. The calibration results are given in Table VI, page 54.

The response of the gage under hydrostatic pressure is illustrated in Figure 30. The hydrostatic response was linear and reproducible with no hysteresis. The sensitivity was also quite satisfactory. The large initial bridge unbalance was caused by a change in resistance of the active arms during bonding to the diaphragm since the balancing resistors were selected in advance based upon the initial resistance of the strain gage.

A representative response curve in soil is given in Figure 31. The nonlinearity and hysteresis for the tests made are less than for diaphragm Model I and more than for diaphragm Model IA (Figure 27, page 76). This behavior appears to be most directly related to the diameter-deflection ratio of the diaphragm (Table V). The range of registration ratios was about the same for Model IB as for Model IA. The average registration ratio for three separate placements in sand for Model IB was 0.95 or a 5 percent underregistration. The results strongly suggest that improved linearity of gage Model IB can be obtained by increasing the diaphragm stiffness further. The gage sensitivity was more than adequate to permit this. However, due to the limitation of funds it was not possible to consider further changes. Four gages of Model IB were fabricated and delivered to AFWL for evaluation.

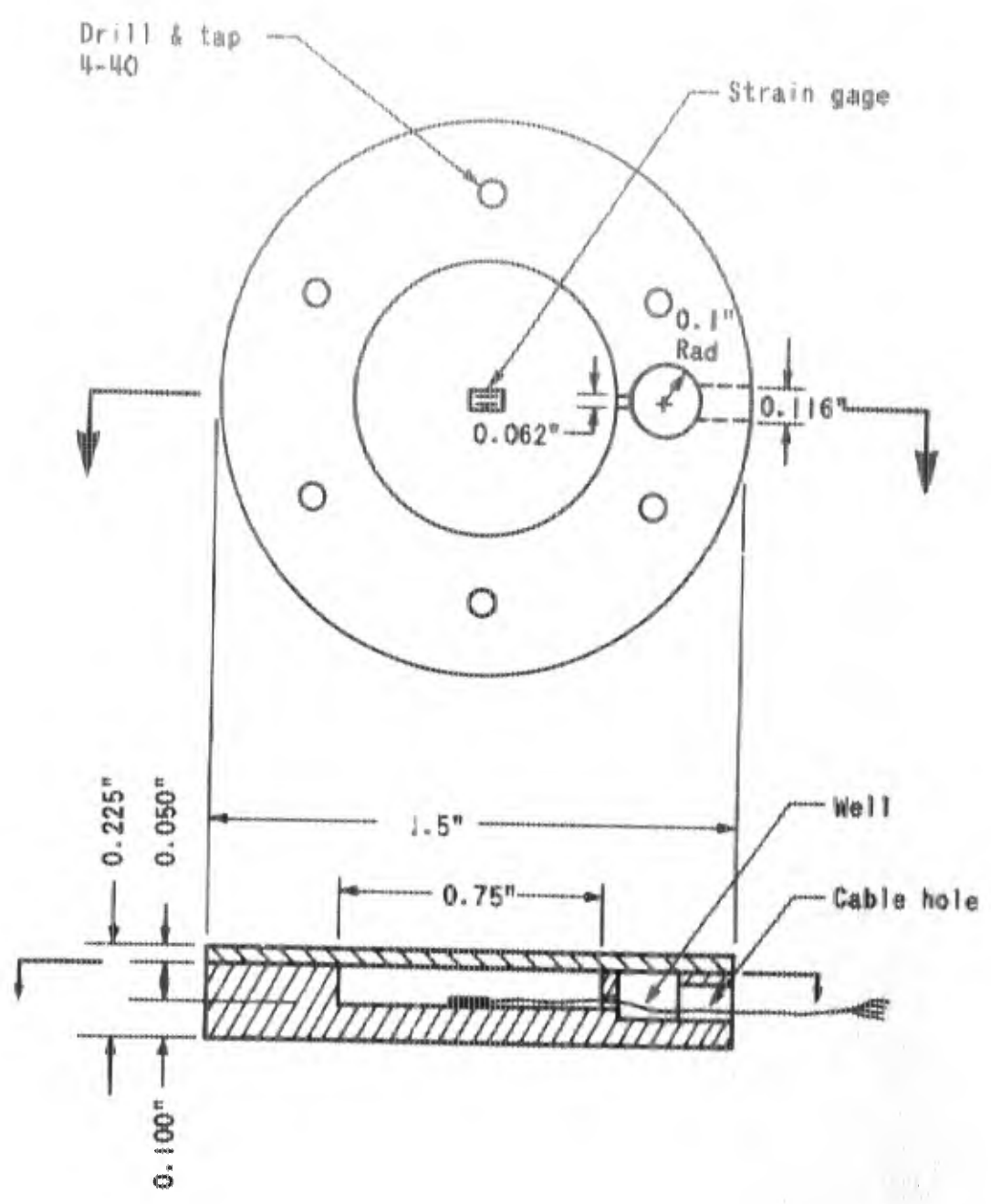


Figure 29. Final Gage Design - Model IB

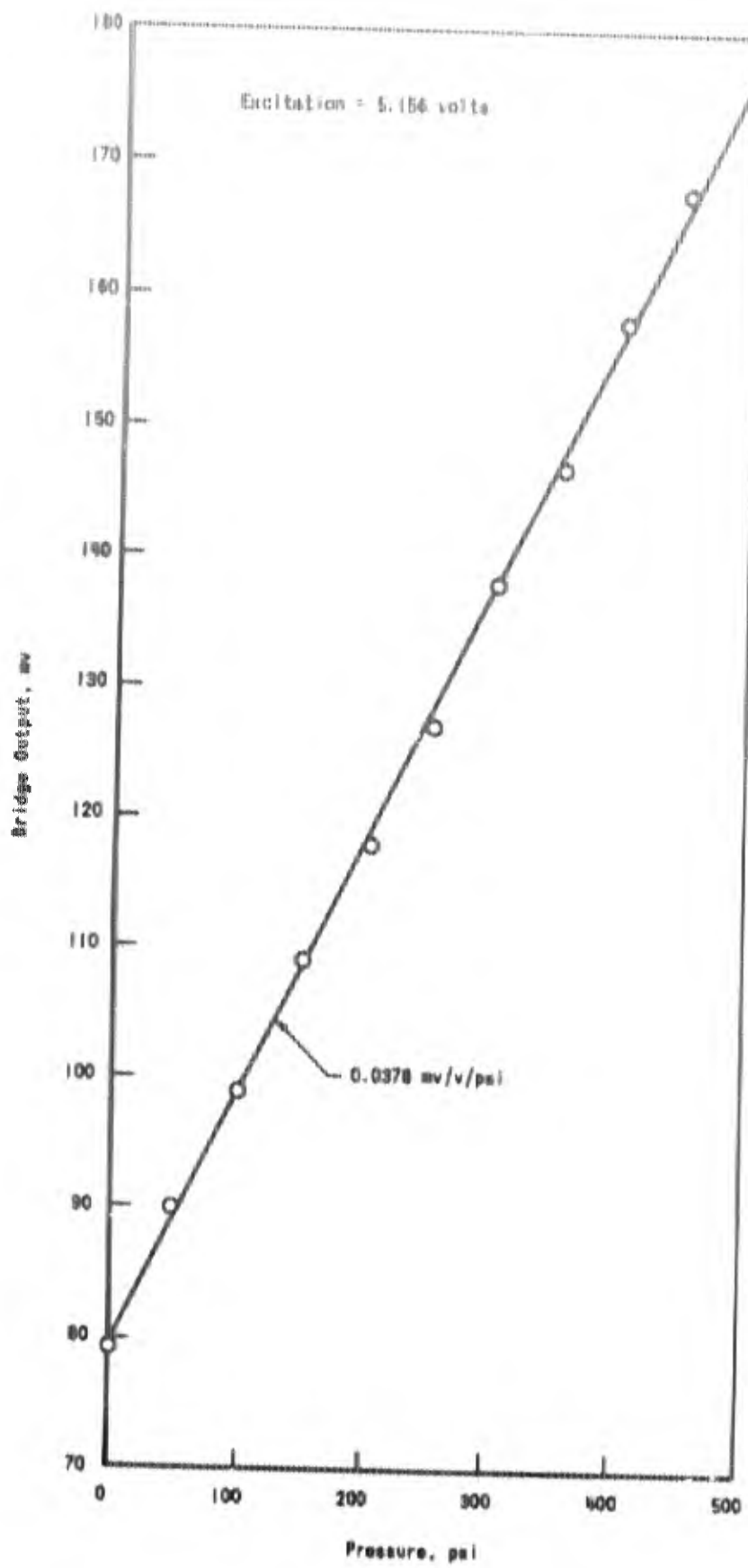


Figure 30. Hydrostatic Calibration of Model IB Diaphragm Gage

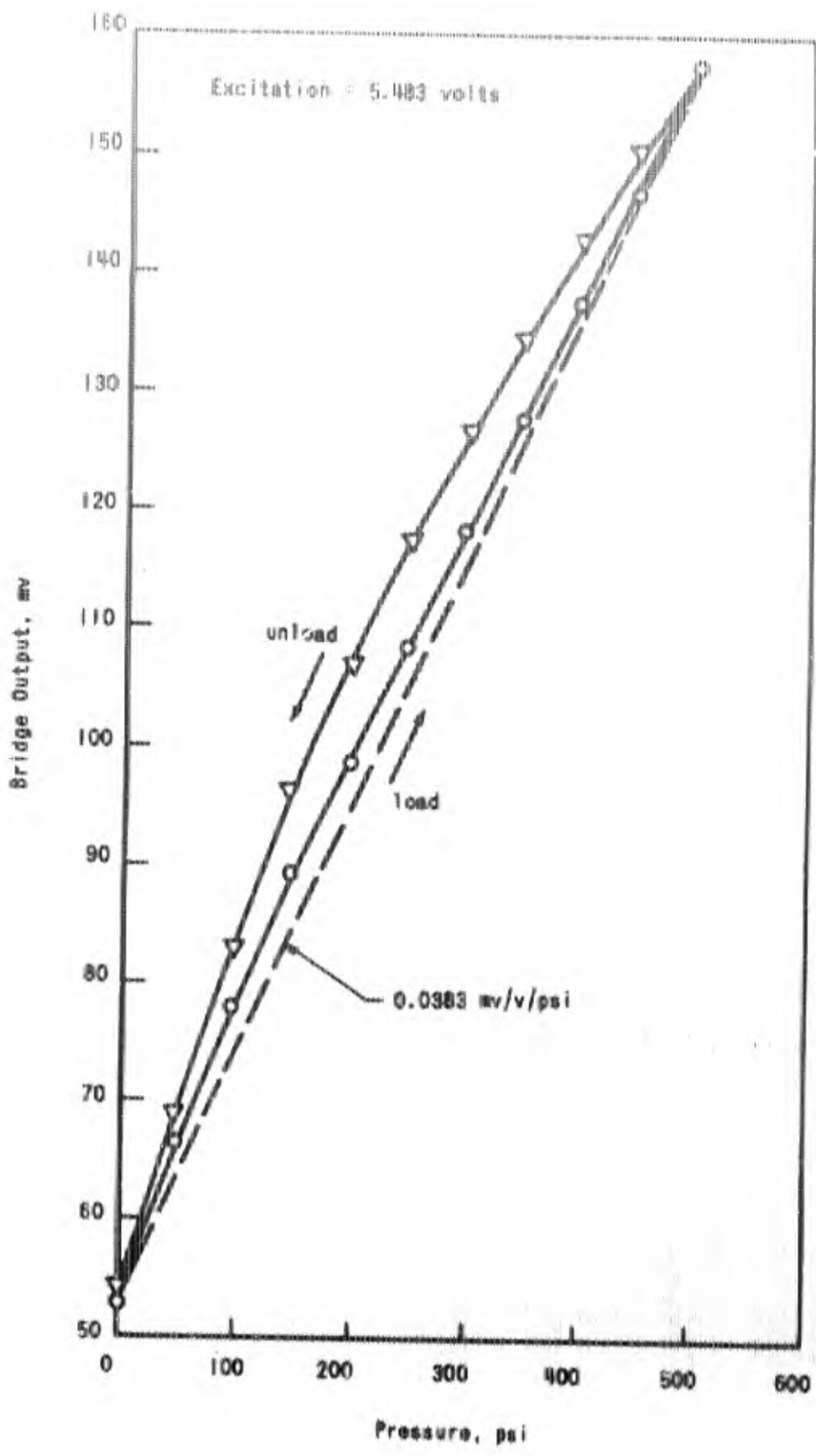


Figure 31. Soil Calibration of Model IB Diaphragm Gage

This page intentionally left blank.

SECTION VII

CONCLUSIONS AND RECOMMENDATIONS

The purpose of this study was to investigate the feasibility of using piezoresistive materials as transducers for soil stress gages. In particular, the potential of utilizing unique properties of solid piezoresistive elements in bending and compression was to be evaluated. Application of commercial piezoresistive strain gage elements as transducers was also to be considered.

A number of gage concepts were evaluated theoretically. Specific gages were then designed embodying three concepts that appeared to be of most interest. The gages were then fabricated and tested both under hydrostatic pressure and in soil up to 500 psi. The results were compared with the performance of the UNM soil stress gage.

The three transducer concepts embodied in the gages evaluated experimentally were: 1) solid piezoresistive elements in direct compression; 2) a beam element with piezoresistive gages attached; and 3) a deflecting diaphragm with piezoresistive strain gages attached.

Theoretically the compression gage appeared to have considerable merit; however, many difficulties in fabricating the gage were encountered. Although considerable effort was devoted to this gage, satisfactory performance was never accomplished. It is believed that these difficulties are not insurmountable; however, additional research will be required to solve the problems.

Mechanical difficulties were encountered with the beam gage. Stress concentrations at the contact point between the beam and the knife edge created nonlinearity and hysteresis during loading and unloading. With further development effort, it is believed that these difficulties can be overcome. However, this concept appears to offer no advantages over other simpler concepts.

The UNM gage varied appreciably in magnitude of response from placement to placement. In general, it appeared to over-register significantly. These characteristics are believed to be primarily a result of the geometry of the gage.

The gage that performed the best used the deflecting diaphragm concept. This gage was also by far the simplest one investigated. The sensitive piezoresistive strain gages have made it possible to use the stiff diaphragms that are necessary to provide satisfactory gage performance in soil. The diaphragm gage has definitely been proven feasible and, considering such factors as simplicity, reliability, and performance in soil, this concept presently appears to be the most satisfactory approach.

The final diaphragm gages developed in the program had a density not much greater than that of soil, a frequency response exceeding 60,000 cps, nonlinearity during loading in soil of less than 5 percent, hysteresis generally less than 8 percent, and registration ratios ranging from 0.84 to 1.05, i.e., from an underregistration of 16 percent to an overregistration of 5 percent. The experimental results indicate that this is not the best performance that can be expected with such gages. It appears that the higher the diameter-to-deflection ratio of the diaphragm the better the linearity and the less the hysteresis in soil. The data also indicate that the smaller the thickness-diameter ratio of the overall gage the closer the gage reads to the true stress. The sensitivity of the final diaphragm gages was considerably greater than the minimum acceptable. Hence, it is possible to further improve the gage performance by sacrificing sensitivity.

The tests conducted have given some indication of the importance of the various design parameters of diaphragm gages on overall gage performance. Some information is also available in the literature on this subject. However, there still remains a significant lack of information on the specific effects of each of the parameters, e.g., thickness-to-diameter ratio, diameter-to-deflection ratio of the diaphragm, and the area of diaphragm in relation to total gage area.

Before any satisfactory basis for design of soil stress gages in general can be provided, a systematic evaluation of the significant parameters, one at a time, must be made in the soil. Because of its simplicity, and because it has been shown to be a feasible concept, the diaphragm gage is ideal for such a study. In addition to the characteristic features of the gage the other variables which should be considered are the soil type, the confining condition of the soil specimen, the placement techniques, and the performance of the gage when oriented in directions other than that of the major principle stress. It is believed that the understanding of stress gage performance in soil currently lags far behind the development of instrumentation techniques, which make it possible now to construct almost any kind of gage that is desired.

The completed program was limited to an investigation of gage concepts which would be useful for the measurement of normal stresses only. Further analytical studies should be carried out to determine material types and orientations that would allow the measurement of other types of stresses. The investigation of new materials other than silicon and germanium should also be pursued. The use of materials with a higher stress sensitivity would enable the stiffness of the gages to be increased without a sacrifice in the available output signal. Higher resistivity along with adequate sensitivity would permit the use of larger solid transducer elements.

The use of noncommercial elements and configurations should also be studied further. The use of diffusion techniques may allow the attainment of high gage factors without concern for the effects of the bonding techniques upon the strain gage performance. Since silicon has approximately the same density as aluminum and soil, it may be possible to design strain gages that would require no metallic cover. Instead, the silicon itself would constitute both the case and the sensing element. The silicon piece could be encapsulated so as to be sufficiently waterproof for use in the field.

BLANK PAGE

SECTION VIII

BIBLIOGRAPHY

1. REFERENCES NOTED IN TEXT

1. Bridgman, F. W., "Effect of Tension on the Transverse and Longitudinal Resistance of Metals", Proceedings of the American Academy of Arts and Sciences; Vol. 60, No. 8, October 1925, p. 423.
2. Smith, Charles S., "Piezoresistive Effect in Germanium and Silicon", Physical Review, Vol. 94, No. 1, April 1, 1954, pp. 42-49.
3. Mason, W. P. and R. N. Thurston, "Use of Piezoresistive Materials in the Measurement of Displacement, Force, and Torque", Journal of the Acous. Soc. of America, Vol. 29, No. 10, October 1957, pp. 1096-1101.
4. Pfann, W. G. and R. N. Thurston, "Semiconducting Stress Transducers Utilizing the Transverse and Shear Piezoresistance Effects", Journal of Applied Physics, Vol. 32, No. 10, October 1961, pp. 2008-2019.
5. Selig, E. T., "A Review of Stress and Strain Measurements in Soil", Proceedings of the Symposium on Soil-Structure Interaction, University of Arizona, Tucson, Arizona, 1964, pp. 172-186.
6. Roark, R. J., "Formulas for Stress and Strain", McGraw-Hill Book Company, Inc., New York, 1943.
7. Shock and Vibration Handbook, C. M. Harris and C. E. Crede, Eds., Vol. I, p. 1-15, McGraw-Hill, New York, 1961.
8. Ingram, J. K., "The Development of a Free-Field Soil Stress Gage for Static and Dynamic Measurements", Symposium on Instrumentation and Apparatus for Soils and Rock, ASTM STP 392, 1965.
9. Stoll, R. D. and I. A. Ebeido, "Shock Waves in Granular Soil", Journal of the Soil Mechanics and Foundations Division, ASCE, Vol. 91, No. SM4, July 1965.

2. OTHER REFERENCES

10. Sion, N., "Pressure Transducers Using Miniature Semiconductor Strain Gages", Industrial Electronics, Vol. 3, Sept. 1965, p. 414.
11. Hollander, L. E., G. L. Vick, and T. J. Diesel, "The Piezoresistive Effect and Its Applications", Rev. of Scientific Inst., Vol. 31, No. 3, March 1960, pp. 323-327.
12. Higson, G. R., "Recent Advances in Strain Gauges", J. Sci. Instrum., Vol. 41, 1964, pp. 405-414.
13. Warschauer, Douglas M., "Black Phosphorous as Strain Gauge and Pressure Transducer", Jour. of Appl. Phys., Vol. 35, No. 12, Dec. 1964, pp. 3516-3519.

DOCUMENT CONTROL DATA - R&D		
<i>(Security classification of title, body of abstract and indexing annotation must be entered when the overall report is classified)</i>		
1. ORIGINATING ACTIVITY (Corporate author) Illinois Institute of Technology Research Institute 10 West 35th Street Chicago, Illinois		2a. REPORT SECURITY CLASSIFICATION Unclassified 2b. GROUP
3. REPORT TITLE PIEZORESISTIVE SOIL STRESS GAGES		
4. DESCRIPTIVE NOTES (Type of report and inclusive dates) Final Report 1 October 1964 to 31 January 1966		
5. AUTHOR(S) (Last name, first name, initial) Selig, Ernest T.; Tobin, Henry G.		
6. REPORT DATE September 1966	7a. TOTAL NO. OF PAGES 108	7b. NO. OF REFS 13
8a. CONTRACT OR GRANT NO. AF29(601)-6628 b. PROJECT NO. 5710 c. Subtask No. 13.166 d.	9a. ORIGINATOR'S REPORT NUMBER(S) AFWL-TR-66-51 9b. OTHER REPORT NO(S) (Any other numbers that may be assigned this report) IITRI Report No. M6094	
10. AVAILABILITY/LIMITATION NOTICES This document is subject to special export controls and each transmittal to foreign governments or foreign nationals may be made only with prior approval of AFWL (WLDC), Kirtland AFB, N.M. Distribution of this document is limited because of the technology discussed.		
11. SUPPLEMENTARY NOTES	12. SPONSORING MILITARY ACTIVITY Air Force Weapons Laboratory (WLDC) Kirtland Air Force Base, New Mexico 87117	
13. ABSTRACT A study was conducted to review the characteristics of available piezoresistive materials and evaluate their suitability as transducers for soil stress gages. The scope was limited to gages for measuring one component of static and dynamic free-field stresses. Three concepts were considered theoretically: 1) piezoresistive strain gage elements mounted on a deflecting diaphragm, 2) solid piezoresistive elements in direct compression and 3) solid piezoresistive beam elements subjected to bending. Gages were designed and fabricated to test each of these concepts. The most satisfactory overall results were obtained with the diaphragm gage. Four such gages were delivered to AFWL in fulfillment of the contract requirements. The compression gage has merit, but there remain many fabrication problems to be overcome. Further effort will be required to develop this concept. The beam gage does not appear as practical as the other types. A systematic study of the behavior of diaphragm gages in soil is one of the most important activities which needs to be undertaken.		

Security Classification

KEY WORDS	LINK A		LINK B		LINK C	
	ROLE	WT	ROLE	WT	ROLE	WT
Soil stress gage						
Piezoresistive						
Diaphragm gage						
Direct compression element						
Bending element						
Normal component of stress						

INSTRUCTIONS

1. **ORIGINATING ACTIVITY:** Enter the name and address of the contractor, subcontractor, grantee, Department of Defense activity or other organization (corporate author) issuing the report.
- 2a. **REPORT SECURITY CLASSIFICATION:** Enter the overall security classification of the report. Indicate whether "Restricted Data" is included. Marking is to be in accordance with appropriate security regulations.
- 2b. **GROUP:** Automatic downgrading is specified in DoD Directive 5200.10 and Armed Forces Industrial Manual. Enter the group number. Also, when applicable, show that optional markings have been used for Group 3 and Group 4 as authorized.
3. **REPORT TITLE:** Enter the complete report title in all capital letters. Titles in all cases should be unclassified. If a meaningful title cannot be selected without classification, show title classification in all capitals in parenthesis immediately following the title.
4. **DESCRIPTIVE NOTES:** If appropriate, enter the type of report, e.g., interim, progress, summary, annual, or final. Give the inclusive dates when a specific reporting period is covered.
5. **AUTHOR(S):** Enter the name(s) of author(s) as shown on or in the report. Enter last name, first name, middle initial. If military, show rank and branch of service. The name of the principal author is an absolute minimum requirement.
6. **REPORT DATE:** Enter the date of the report as day, month, year, or month, year. If more than one date appears on the report, use date of publication.
- 7a. **TOTAL NUMBER OF PAGES:** The total page count should follow normal pagination procedures, i.e., enter the number of pages containing information.
- 7b. **NUMBER OF REFERENCES:** Enter the total number of references cited in the report.
- 8a. **CONTRACT OR GRANT NUMBER:** If appropriate, enter the applicable number of the contract or grant under which the report was written.
- 8b, 8c, & 8d. **PROJECT NUMBER:** Enter the appropriate military department identification, such as project number, subproject number, system numbers, task number, etc.
- 9a. **ORIGINATOR'S REPORT NUMBER(S):** Enter the official report number by which the document will be identified and controlled by the originating activity. This number must be unique to this report.
- 9b. **OTHER REPORT NUMBER(S):** If the report has been assigned any other report numbers (either by the originator or by the sponsor), also enter this number(s).
10. **AVAILABILITY/LIMITATION NOTICES:** Enter any limitations on further dissemination of the report, other than those

imposed by security classification, using standard statements such as:

- (1) "Qualified requesters may obtain copies of this report from DDC."
- (2) "Foreign announcement and dissemination of this report by DDC is not authorized."
- (3) "U. S. Government agencies may obtain copies of this report directly from DDC. Other qualified DDC users shall request through _____."
- (4) "U. S. military agencies may obtain copies of this report directly from DDC. Other qualified users shall request through _____."
- (5) "All distribution of this report is controlled. Qualified DDC users shall request through _____."

If the report has been furnished to the Office of Technical Services, Department of Commerce, for sale to the public, indicate this fact and enter the price, if known.

11. **SUPPLEMENTARY NOTES:** Use for additional explanatory notes.
12. **SPONSORING MILITARY ACTIVITY:** Enter the name of the departmental project office or laboratory sponsoring (paying for) the research and development. Include address.
13. **ABSTRACT:** Enter an abstract giving a brief and actual summary of the document indicative of the report, even though it may also appear elsewhere in the body of the technical report. If additional space is required, a continuation sheet shall be attached.

It is highly desirable that the abstract of classified reports be unclassified. Each paragraph of the abstract shall end with an indication of the military security classification of the information in the paragraph, represented as (TS), (S), (C), or (U).

There is no limitation on the length of the abstract. However, the suggested length is from 150 to 225 words.

14. **KEY WORDS:** Key words are technically meaningful terms or short phrases that characterize a report and may be used as index entries for cataloging the report. Key words must be selected so that no security classification is required. Identifiers, such as equipment model designation, trade name, military project code name, geographic location, may be used as key words but will be followed by an indication of technical context. The assignment of links, rules, and weights is optional.